IEEE Access
Multidisciplinary | Rapid Review | Open Access Journal

Received June 29, 2021, accepted July 12, 2021, date of publication July 21, 2021, date of current version August 4, 2021.

Digital Object Identifier 10.1109/ACCESS.2021.3099027

Closed-Loop Cognitive Stress Regulation Using Fuzzy Control in Wearable-Machine Interface Architectures

HAMID FEKRI AZGOMI[1], (Student Member, IEEE), IAHN CAJIGAS[2], (Member, IEEE), AND ROSE T. FAGHIH[1], (Member, IEEE)

[1]Department of Electrical and Computer Engineering, University of Houston Cullen College of Engineering, Houston, TX 77004, USA
[2]Department of Neurological Surgery, University of Miami Miller School of Medicine, Miami, FL 33136, USA

Corresponding author: Rose T. Faghih (rtfaghih@uh.edu)

This work was supported in part by NSF CAREER Award through Multimodal Intelligent Noninvasive brain state Decoder for Wearable AdapTive Closed-loop arcHitectures (MINDWATCH) under Grant 1942585, and in part by NSF Grant through Wearable-Machine Interface Architectures [Computer and Information Science and Engineering (CISE) Research Initiation Initiative (CRII): cyber-physical system (CPS)] under Grant 1755780. Rose T. Faghih served as the senior author.

This work involved human subjects or animals in its research. The authors confirm that all human/animal subject research procedures and protocols are exempt from review board approval.

ABSTRACT Keeping cognitive stress at a healthy range can improve the overall quality of life: helping subjects to decrease their high levels of arousal, which will make them relaxed, and elevate their low levels of arousal, which could increase their engagement. With recent advances in wearable technologies, collected skin conductance data provides us with valuable information regarding ones' cognitive stress-related state. In this research, we aim to create a simulation environment to control a cognitive stress-related state in a closed-loop manner. Toward this goal, by analyzing the collected skin conductance data from different subjects, we model skin conductance response events as a function of simulated environmental stimuli associated with cognitive stress and relaxation. Then, we estimate the hidden stress-related state by employing Bayesian filtering. Finally, we design a fuzzy control structure to close the loop in the simulation environment. Particularly, we design two classes of controllers: (1) an inhibitory controller for reducing cognitive stress and (2) an excitatory controller for increasing cognitive stress. We extend our previous work by implementing the proposed approach on multiple subjects' profiles. Final results confirm that our simulated skin conductance responses are in agreement with experimental data. In a simulation study based on experimental data, we illustrate the feasibility of designing both excitatory and inhibitory closed-loop wearable-machine interface architectures to regulate the estimated cognitive stress state. Due to the increased ubiquity of wearable devices capable of measuring cognitive stress-related variables, the proposed architecture is an initial step to treating cognitive disorders using non-invasive brain state decoding.

INDEX TERMS Bayesian filter, closed-loop systems, cognitive stress, fuzzy control, skin conductance.

I. INTRODUCTION

Stress-related health issues attract massive attention in the modern world [1], [2]. Despite recent advances in technology, handling cognitive stress-related disorders is still a major problem around the globe and impacts quality of life in general [3]. Additionally, low levels of eustress, or positive cognitive stress, could negatively affects work productivity [4]. Experiencing high levels of cognitive stress while performing routines, or low cognitive engagement with the environment, may seriously affect an individual's life [5]. Over 60% of Americans feel that stress negatively affects their work performance [6]. Considering the fact that the brain performs better when internal cognitive stress state is within a moderate range [7], stress regulation has recently received a lot of attention. Fig. 1 depicts the relationship between performance and the amount of stress that a person encounters. As depicted in Fig. 1, the performance is at its peak when the stress level is within a normal range [4]. While there exist methods for managing stress, there is still a lack of reliable systems that continuously track the stress levels in individuals and automatically regulate stress levels by suggesting appropriate non-invasive solutions during daily activities [8], [9].

The associate editor coordinating the review of this manuscript and approving it for publication was Haibin Sun.

This work is licensed under a Creative Commons Attribution 4.0 License. For more information, see https://creativecommons.org/licenses/by/4.0/

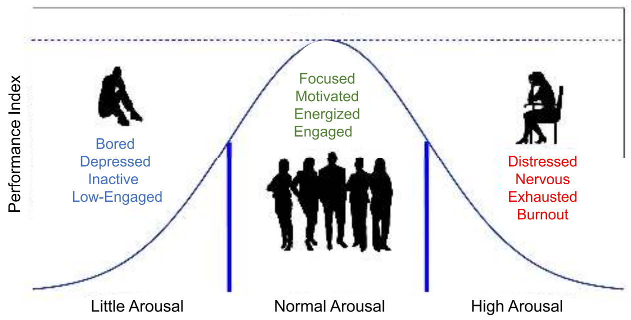

FIGURE 1. Arousal-performance curve. While high amount of arousal (stress) may cause nervousness, too little amount of arousal (stress) may negatively affects productivity and bring the person about feeling bored and inactive. Eustress or good type of stress will cause the person to be focused, more productive, and better engaged with the environment [4].

The human brain detects and mediates the physiologic response to environmental stimuli including cognitive stress tasks [10]. Traditional approaches that try to directly monitor brain activity (e.g., using electroencephalogram (EEG) signal [11]) are neither comfortable nor practical in daily life [12]. Thanks to the recent advances in wrist-worn wearable device technologies, we now have the opportunity to easily monitor various physiological signals and understand brain activity [13]–[16]. To infer internal stress state, rather than monitoring the brain activity directly, one might be able to collect measurements that correspond to the hidden stress state using the wearable devices [17]–[23].

Among the data that can be collected via wearable devices, skin conductance data carries important information about the brain's cognitive stress [24]–[28]. Cognitive stress can be inferred from the tone of the sympathetic nervous system (or "fight or flight" response system). The sympathetic nervous system is a branch of the automatic nervous system (ANS) [29]. Since Electrodermal activity (EDA) does not include any representation of the parasympathetic nervous system (i.e., another branch of ANS), it is a suitable representative for cognitive stress analysis [30], [31]. While heart rate also provides insight about the internal arousal state, it carries information associated with cardiac activity [29], [32]. As skin conductance signal provides information about sympathetic nervous system, we focus on this physiological signal for further analysis [33]. In the presence of external (e.g., environmental) or internal (e.g., mental) stimulus, there are small variations in the activity of the sweat glands [34]. Consequently, electrical characteristics of the skin will change. Such fluctuations are indicated in the skin conductance response (SCR), which can be measured using wearable devices [18], [21], [28].

That the SCR rate encodes stress-related information (i.e., more stress is associated with the increased SCR and vice versa) has been validated in experimental studies [21], [26], [35]. In addition to the studies related to inferring brain activity using skin conductance signal [28], [34], [36], there exist research that employ this biomarker as a reference signal [37]–[39]. For instance, Lee *et al.* use motion sensors to classify the stress level and employ skin conductance as a reference for stress detection [40]. Perry *et al.* designed a wearable device that can determine stress levels by monitoring the amount of cortisol that is present in human's sweat [41]. In this research, we relate the internal cognitive stress state to the changes in skin conductance signal.

Compared to available methods that try to detect stress and send an alert to the person [42], [43], our goal here is to track stress levels in a continuous manner and design a control strategy to regulate the cognitive stress by a non-invasive approach in a simulation environment. Rachakonda *et al.* used physiological data such as respiration, heart rate and skin conductance, and then, by incorporating machine learning algorithms, they performed a classification method on the stress levels [44]. The results demonstrate classifications for particular stress ranges. Similarly, Sano *et al.* have employed machine learning tools on the collected physiological signals (i.e., accelerometer and skin conductance data), mobile data such as text and call, and the surveys completed by the subjects to perform stress range classification [16]. Compared to the majority of research being done in this area, which employ machine learning approaches to classify the stress levels [45]–[47], the proposed state-space method would lead us to track stress severity as a continuous value in real-time. This will further provide the chance to better design the actuation policy for closing the loop and keeping the stress state within a desired range. Moreover, continuously tracking of cognitive stress might help the person to increase eustress [48]. Hence, following the proposed architecture, we would be able to track subject's cognitive stress as a continuous state and design the control mechanism to keep this hidden state within a desired range.

In recent years, there have been several studies dealing with closed-loop approaches [49]–[54]. Walter *et al.* classified workload in an adaptive learning environment [54]. They proposed to track mental workload using the EEG signal and design the course material to close the loop and increase the efficiency. Utilizing our proposed approach, one would be able to track the internal stress state continuously and design the required actuation accordingly. This actuation could be any changes in the workload, changing light colors and frequencies in workplaces, listening to music, drinking excitatory or relaxing beverages, or designing the break time based on internal stress levels to keep them within desired range. In this research, we propose to use wearable-machine interface (WMI) architectures to control the cognitive stress-related state in a simulation environment. As presented in Fig. 2, the architecture includes collecting physiological signals using a wearable device, inferring neural stimuli underlying pulsatile SCR events, estimating an unobserved stress-related state from underlying neural stimuli, designing the control, and closing the loop to regulate subject's cognitive stress state and keep it within a desired range in a real-time manner [1].

This article has been accepted for publication in a future issue of this journal, but has not been fully edited. Content may change prior to final publication. Citation information: DOI 10.1109/ACCESS.2021.3099027, IEEE Access

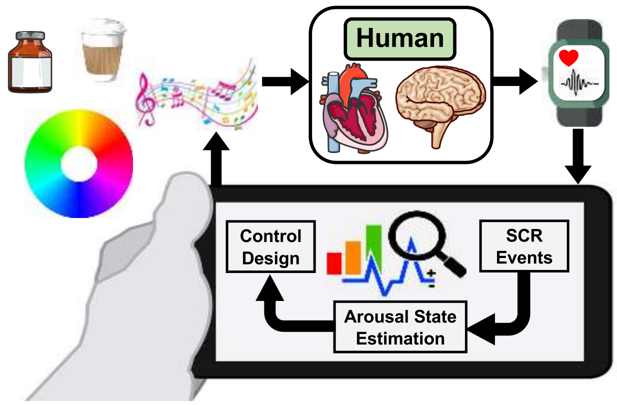

FIGURE 2. **Wearable machine interface architecture. A wrist-worn wearable device is employed to monitor and measure corresponding physiological data from the human in the loop. Then, by analyzing the data and inferring the body's internal activity, a decoder estimates the stress state. Finally, the controller provides the required control input to maintain aforementioned state within a desired range. The ultimate goal of this WMI architecture is to employ different non-invasive actuation such as music, drink, and changing the lights, to close the loop in real-world.**

Taking advantage of the real-time simulation model, we present our approach in designing the control algorithm and closing the loop in a systematic way. We employ fuzzy logic, as a knowledge-based control approach, to control cognitive stress state in a simulation environment [55], [56]. The knowledge-based control approaches make inference and design the control action using the insight achieved from system dynamics. The fuzzy logic controller employs insights about the system, performs inference, and derives the actuation policy [57], [58]. Researchers in [55] assume that all the states are available while designing the control system. Zhang *et al.* employ a fuzzy adaptive state observer to estimate the hidden state and design a fuzzy controller to close the loop [58]. Their proposed approach is effective when dealing with unknown control directions [58].

In this *in silico* study, we present a simulation setting to show how an automated control action will result in regulation of both modeled SCR events and the estimated cognitive stress-related state. Toward this aim, we relate the internal stress state to the changes in SCR events. By estimating the hidden stress-related state and designing the control action, we close the loop in real-time. More specifically, we consider one open-loop, one closed-loop inhibitory, and one closed-loop excitatory examples to demonstrate the performance of our proposed WMI architecture in different simulation scenarios. The final results verify that the proposed architecture not only can successfully track one's cognitive stress state, but also that the control mechanism is effective in both excitation and inhibition applications in real-time. The present *in silico* study based on experimental data is one of the very first attempts to build a real-time environment to further investigate the effects of modern control techniques in regulating internal arousal state. The main contributions of this research are summarized as follows.

- Building a simulation environment based on experimental data from wearable devices to relate the changes in skin conductance signal to one's internal arousal state.
- Simulating the required environmental stimuli functions for both high and low arousal sessions.
- Real-time and continuous tracking of the internal arousal state in response to the changes in the environmental stimuli via state-space methods and Bayesian estimation in the simulation framework.
- Estimating an internal arousal state based on peripheral physiological data that are collected using wearable devices, rather than directly monitoring of brain activity.
- Presenting a novel framework suitable to investigate the effects of various noninvasive strategies to regulate the internal stress-related state.
- Implementing a straightforward fuzzy controller to take advantage of the open-loop simulation results and regulating the estimated arousal state in both inhibitory and excitatory class of closed-loop systems.

II. METHODS

Fig. 3 illustrates an overview of the present research paradigm. The proposed procedure consists of two main parts: the offline process and the real-time closed-loop simulation system. In the offline process prior to the real-time implementation, we aim to build a simulation environment based on the experimental measurements [12] (red box in panel (A) of Fig. 3). To this end, we focus on the collected skin conductance data from subjects during a cognitive stress task followed by a relaxation period. Performing deconvolution on skin conductance data, we take the information regarding the number, timings, and amplitudes of underlying neural stimuli associated with SCR [21], [26]. A brief description of the employed deconvolution algorithm is presented in Appendix A [21]. By binarizing the neural impulses, and employing a state-space approach, we follow the methods presented in [26], [27], [59] and relate the internal cognitive stress-related state to the underlying neural impulses. Incorporating Bayesian filtering with an Expectation Maximization (EM) algorithm, we estimate the hidden cognitive stress-related state in an offline manner.

To design the real-time simulation environment, we take the estimated cognitive stress state as the output of the offline process and model the required environmental stimuli responsible for the changes in estimated state trajectory. Then, we generate two different sets of stimuli: one for causing low arousal (relaxation), and one for inducing high arousal (cognitive stress). Next, in a real-time simulation environment, we relate a cognitive stress-related state to the simulated SCR events using a state-space approach. We assume that the probability of receiving the SCR events follows a Bernoulli distribution. We estimate the hidden stress-related state using Bayesian filtering. To close the loop and regulate the estimated cognitive stress-related state in the simulation environment, we design a fuzzy control algorithm to derive essential control signals in real-time. In this research,

This article has been accepted for publication in a future issue of this journal, but has not been fully edited. Content may change prior to final publication. Citation information: DOI 10.1109/ACCESS.2021.3099027, IEEE Access

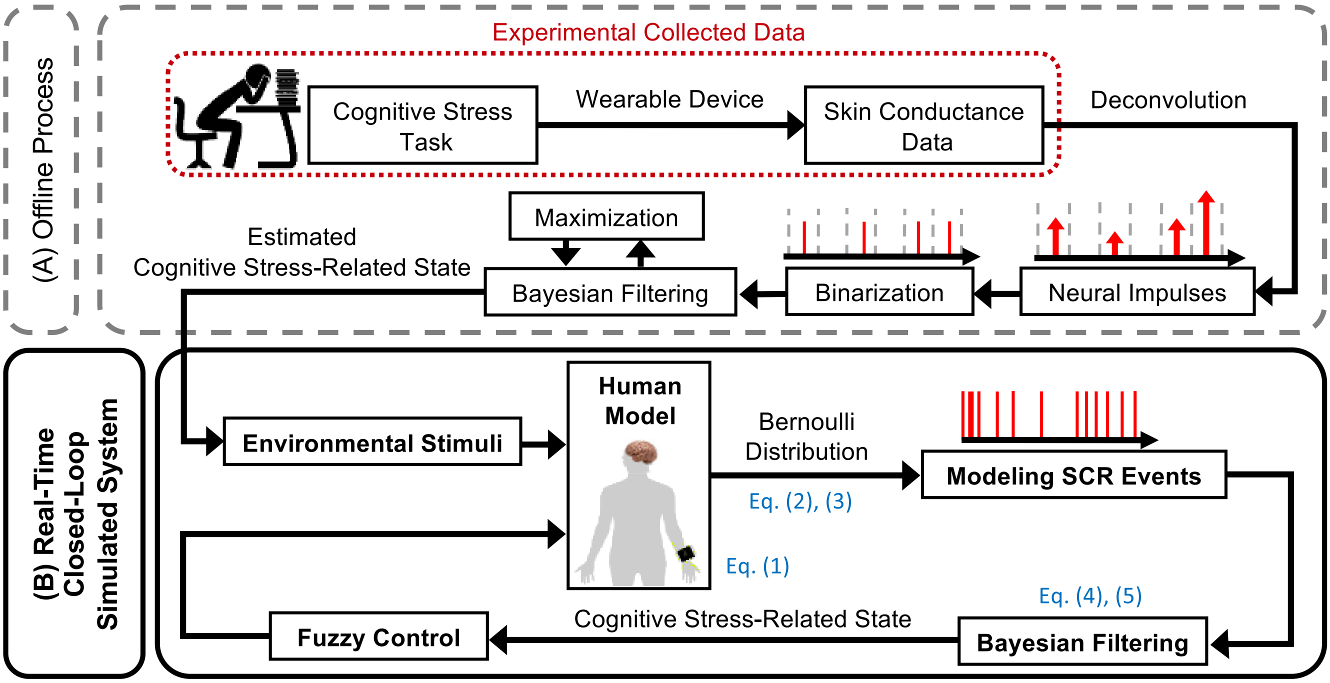

FIGURE 3. Real-time closed-loop system. The dashed box implies the offline process (A) and the solid box depicts the real-time closed-loop system (B). In the offline process, based on the recorded data, while the subjects experience cognitive stress task, a wearable device has measured their skin conductance data. First, we perform the deconvolution, extract the neural impulses and binarize them. Then, by employing Bayesian filtering and Expectation Maximization (EM), a decoder estimates the cognitive stress-related state. To close the loop in real-time, by analyzing different subjects' estimated stress state, we model the corresponding environmental stimuli for each subject. In a state-space representation, human model simulates the skin conductance response (SCR) events by a Bernoulli distribution. Then, using Bayesian filtering approach, the cognitive stress-related state is estimated in real-time. Fuzzy controller takes the estimated stress state and regulates it with the derived control action in a closed-loop manner.

we extend our primary results presented in [1] and implement the proposed WMI architecture on multiple subjects' simulated profiles [26], [27].

A. EXPERIMENTAL COLLECTED DATA DESCRIPTION

In this study, we focus on the Non-EEG Dataset for Assessment of Neurological Status [12] which is publicly available in the PhysioNet database [60]. In this experiment, twenty college students were subjected to different tasks: physical stress, cognitive stress, emotional stress followed by a relaxation period [12]. With the goal of investigating human responses to different types of stress, they have collected skin conductance, body temperature, and 3D accelerometer signals using the Affectiva Q Curve wearable device [12]. In addition, they have collected heart rate and blood oxygenation by the Nonin Wireless WristOx2 oximeter [12]. Among all of the collected physiological signals, it has been shown that SCR, which reflects changes in the sweat gland activities, carry important information regarding sympathetic nervous system arousal [17], [21], [26], [28], [38], [61]. Toward the goal of creating a closed-loop simulation environment for cognitive stress regulation, we extract skin conductance data that corresponds to the cognitive stress task and the relaxation periods [12], [26], [27].

The cognitive stress task in this experiment consists of an arithmetic task (i.e., counting backward by sevens, starting with 2485) for three minutes and the Stroop test (i.e., reading words including a color's name written in a different color ink and indicating the color ink) for two minutes. This arithmetic stress task is a good representative for the cognitive stressor [62]. In the relaxation task, subjects are asked to sit and listen to relaxing music. In the relaxation period, subjects have listened to a portion of *Binaural*, (i.e, a soothing music used in meditation [63], [64]). As the arithmetic task and the relaxation period are considered as the most representative cases, we select on these two parts to show the feasibility on the most extreme arousal scenarios (i.e., high arousal vs low arousal [1]). In other words, we investigate these two parts of data to get insight about how the brain will respond during extreme cases. Skin conductance signal can be contaminated by measurement noise sources such as motion artifacts, range saturation and amplification factor changes [65]. Since the present work builds on a previously published dataset [21], [26]–[28], highly noisy data was discarded prior to further processing. In our previous work [1], we utilized the proposed architecture on only one subject and now we extend it to all selected participants [1], [26]. Selected subjects' information is presented in Table 1.

B. HUMAN BRAIN STIMULUS-RESPONSE MODEL

To model human brain responses, we use the state-space approach and assume that the hidden cognitive stress-related

TABLE 1. Selected subjects' information.

Participants	Subjects ID	Gender	Age	Height [cm]	Weight [kg]
1	1	M	30	177	94
2	5	M	30	182	82
3	8	M	27	182	64
4	9	M	25	177	68
5	12	F	32	162	53
6	16	M	24	180	54

state is affected by the environmental stimuli [26]:

$$x_{k+1} = x_k + u_k + \eta_k \tag{1}$$

where x_k is the hidden cognitive stress-related state, u_k is the control signal, $\eta_k = s_k + \nu_k$ is the environmental input, s_k is the environmental stimuli with the process noise $\nu_k \sim \mathcal{N}(0, \sigma_\nu^2)$ at kth time step. [27], [61]. Similar to [26], [27], we assume the probability of receiving SCR events follows a Bernoulli distribution:

$$P(n_k|x_k) = q_k^{n_k}(1 - q_k)^{1-n_k} \tag{2}$$

To relate probability q_k of observing a SCR event n_k (i.e., a binary value in (2)) to the stress state x_k, we employ the following Sigmoid function:

$$q_k = \frac{1}{1 + e^{-(\beta + x_k)}} \tag{3}$$

where β is the person-specific baseline parameter. To derive β, we define the baseline state of the subject as zero ($x_0 = 0$) and look at changes from this baseline state. Then, we calculate β based on the average probability of an SCR occurring in the whole data $\left(\beta = log(\frac{q_0}{1-q_0}) - x_0\right)$ [26].

C. COGNITIVE STRESS STATE ESTIMATION

To estimate the hidden cognitive stress-related state, we follow the state estimation framework presented in [26], [27]. For the sake of completeness, we briefly review the methodology and employ it for further analysis. Given the simulated SCR events n_k, we estimate hidden state x_k and its corresponding variance term σ_k^2. At this stage of the offline process, we ignore environmental stimuli term, η_k, in (1):

$$\hat{x}_k = \hat{x}_{k-1} + (\hat{\sigma}_{k-1}^2 + \sigma_\nu^2)\Big(n_k - \frac{1}{1 + e^{-(\beta + \hat{x}_k)}}\Big) \tag{4}$$

$$\hat{\sigma}_k^2 = \Big(\frac{1}{\hat{\sigma}_{k-1}^2 + \sigma_\nu^2} + \frac{e^{(\beta + \hat{x}_k)}}{(1 + e^{(\beta + \hat{x}_k)})^2}\Big)^{-1} \tag{5}$$

where $\hat{x}_k$ and $\hat{\sigma}_k^2$ are the estimated hidden cognitive stress-related state and its variance, respectively. We use the EM algorithm presented in [26], [27] to find the σ_ν^2 in (1) and initial values (i.e., x_0 and σ_0^2). The details of EM algorithm can be found in [59], [66]. It should be noted that $\hat{x}_k$ observed on both sides of (4) results in a nonlinear equation. Hence, Newton's method is employed to solve update equations. While for control design we only focus on cognitive stress (as the high arousal representative) and relaxation (as the low arousal representative) periods, we present the results of implementing the same modeling and estimation algorithms on the whole experiment in [12] to show the accuracy and the adequacy of proposed approach (see Fig. 4). To this end, we follow the results provided in [26], [27].

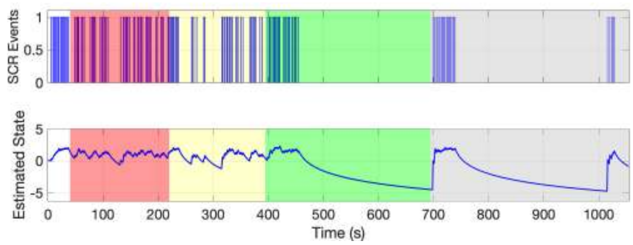

FIGURE 4. Offline arousal state estimation and the corresponding SCR events for multiple tasks. The top panel and the bottom panel show the SCR events and the estimated arousal state, respectively. The shaded backgrounds correspond in turn to the instruction for cognitive stress task (white), arithmetic task (red), Stroop test (yellow), relaxation (green), and emotional stress (grey). Both arithmetic task and Stroop test are associated with the cognitive stress period [26], [27].

D. ENVIRONMENTAL STIMULI MODEL

As presented in Fig. 3, to design the real-time simulation environment, we model the environmental stimuli which is responsible for the fluctuations in estimated stress state. It is worth mentioning that in case of real-world settings, SCR events are obtained via deconvolving measured skin conductance signal [18], [21], [28] in a real-time manner. Analyzing the estimated stress-related state in both cognitive stress and relaxation tasks in the offline process, we aim to find the required environmental stimuli for both sessions. Examining the open-loop system and considering there is no control in (1) (i.e., $u_k = 0$), we derive $\eta_k = s_k + \nu_k = x_k - x_{k-1}$. Where x_k is the estimated cognitive stress-related state in the offline stage. By ignoring the process noise in this stage, we find time series for the target environmental stimuli s_k:

$$\begin{pmatrix} s_1 \\ s_2 \\ \vdots \\ s_T \end{pmatrix} = \begin{pmatrix} x_1 - x_0 \\ x_2 - x_1 \\ \vdots \\ x_T - x_{T-1} \end{pmatrix} \tag{6}$$

Investigating the offline open-loop results on all selected subjects, we analyze the general trend in s_k. To simulate a general environmental stimuli function s_k responsible for the changes in cognitive stress session, we consider the summation of sinusoidal harmonic functions. We also assume the behaviour of s_k in the relaxation period follows an exponential decay [1]. These assumptions are made to simplify solving the optimization problems and generating the environmental stimuli. Hence, we consider two environmental stimuli models: one for the cognitive stress task s_k^c, and one for the relaxation period s_k^r. We assume $s_k^c = \sum_{n=1}^{N} \alpha_n \cos(\omega_n k + \gamma_n)$, where N is the number of the harmonics, and α_n, ω_n, and γ_n for $n = 1, \ldots, N$ are the amplitude, frequency, and phase shift of each of the harmonics, respectively. Performing spectral analysis on each participant, we find the

This article has been accepted for publication in a future issue of this journal, but has not been fully edited. Content may change prior to final publication. Citation information: DOI 10.1109/ACCESS.2021.3099027, IEEE Access

optimal number of harmonics N needed for estimating the high arousal stimuli. The regression parameters are estimated using a least square approach [67]. Similarly, for relaxation period, we assume an exponential decay as the environmental forcing function. More specifically, we let $s_k^r = ae^{bk}$ where the regression parameters a and b are being derived using least square regression method.

It should also pointed out that any changes to these assumptions (i.e., sinusoidal harmonics for high arousal, and exponential decay for low arousal) would change the resulted environmental stimuli functions. However, in real-world implementation of the proposed approach, by monitoring the skin conductance signal and performing the deconvolution algorithm on the captured signal, there is no need to apply these simulated environment functions.

By extracting the environmental stimuli associated with both high and low arousal, and including the process noise, ν_k, we incorporate them in the state-space model (1) and build the simulation model. Consequently, we run the whole simulation system in both open-loop (i.e., $u_k = 0$) and closed-loop (i.e., $u_k \neq 0$) scenarios.

E. CONTROL DESIGN

Analyzing the system's open-loop behaviour in the simulation environment leads us to design the fuzzy structure including the membership functions, defuzzification, and inference engine [68]. We use the simulated environmental stimuli for both high and low arousal sessions and obtain the required knowledge about the system behavior in an open-loop manner. In the simulation environment, the human brain model generates SCR events in response to the various environmental stimuli. As a result, we see how the estimated stress state will fluctuate in response the changes in external environmental stimuli. This feature of incorporating insights about the system while designing the control structure is the main reason for choosing the fuzzy control.

In the proposed architecture, the real-time estimated cognitive stress-related state x_k is the input and the control signal u_k in (1) is the output of the fuzzy system. The heart of any fuzzy system, is its rule base. These rules are based on the constraints and insight about the system dynamics. To build a rule base applicable for multiple subjects, we form the rules as follows:

- If the estimated cognitive state is *low arousal*, then control is *excitatory*.
- If the estimated cognitive state is *neutral*, then control is *neutral*.
- If the estimated cognitive state is *high arousal*, then control is *inhibitory*.

To convert the linguistic variables presented in the rule base to the crisp values, we impose the membership functions. These membership functions for both input and output values are depicted in Fig. 5. As presented in top-panel of Fig. 5, the input membership functions of the fuzzy system, which are related to the stress state, include three sets of functions;

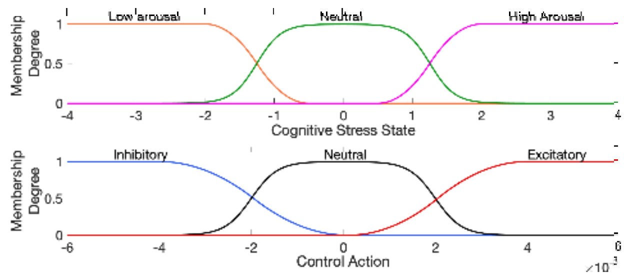

FIGURE 5. Input and output membership functions. The top-panel shows the membership functions for the input (i.e., estimated cognitive stress-related state x_k). The bottom-panel shows the membership functions for the output (i.e., control signal u_k).

TABLE 2. Input and output membership functions (Fig. 5).

Variable	Membership Function	Category
$\mu(x_k)$	$zmf(x_k, -2, 0.5)$ $psigmf(x_k, 5.6, -1.2, -5.6, 1.2)$ $smf(x_k, 0.5, 2)$	Low arousal Neutral High arousal
$\mu(u_k)$	$zmf(u_k, -0.004, 0.0001)$ $psigmf(u_k, 3500, -0.002, -3500, 0.002)$ $smf(u_k, 0.0001, 0.004)$	Inhibitory Neutral Excitatory

low arousal, neutral, and high arousal. The output of the fuzzy system, which is the control signal, consists of three sets; inhibitory, neutral, and excitatory (bottom-panel of Fig. 5). The membership functions presented in Fig. 5 are described in Table 2.

According to the rule base, once the system detects the high arousal, we need to have inhibitory control to decrease the number of SCR events and lower the stress state. On the other hand, when we deal with the low levels of cognitive stress state, we need excitation control to increase the number of SCR events and elevate the stress-related state. Similar to [1], we use *Mamdani engine* and *centroid* method for inference and defuzzification, respectively [56], [58].

F. STABILITY ANALYSIS

According to the state-space model (1) and nonlinear stochastic observation (2), similar to any control technique, global stability could not be guaranteed within the proposed control approach [69]. However, by following the recent approaches that handle the stability analysis for control of probabilistic models [70], we aim to calculate a stability region. It will ensure that the state trajectory will be converged to the target levels in a finite time horizon [71]. In this approach, taking advantage of the simulation environment, as well as the real-time estimate of state mean, $\hat{x}_k$, we analyze the performance of the closed-loop system in response to multiple initial starting point, x_0, and derive the stability region [70].

According to Lyapunov's stability theory, the target point x^d is stable, if for any $\epsilon > 0$, there exists $\delta > 0$, such that $||x_k - x^d|| < \epsilon$ and $||x_0 - x^d|| < \delta$. A stability region, X^s, denotes to a subset in which $||x_k - x^d|| \to 0$ for all $x_0 \in X^s$ as $k \to \infty$. Here, we aim to obtain such a region which would guarantee that the difference between the current state and the target levels would be decreased as time evolves:

$$||x_k - x^d|| < \zeta\, ||x_{k-1} - x^d|| \tag{7}$$

for a fixed $\zeta < 1$. According to the positively invariant sets [70], [72], once the state transition starts within the calculated region (i.e., $x_0 \in X^s$) and (7) holds, it will never leave it.

G. ALGORITHM

To summarize all the steps required for establishing the simulation environment and regulating the cognitive stress state in a closed-loop manner (Fig. 3), we present the following algorithm:

Algorithm 1 Offline Process and Real-Time Closed-Loop System Design (Fig. 3)

Offline Stage

(a) Analyze the experimental skin conductance data and extract the sessions associated with the cognitive stress and relaxation (i.e., $y_{SC}(t)$ in (8)).
(b) Employ cvxEDA toolbox [73] to extract the phasic part from the skin conductance signal (i.e., $y_P(t)$ in (8)).
(c) Sample the phasic part signal and perform deconvolution algorithm to infer the brain neural impulses and estimate model parameters (i.e., θ and $\mathbf{u}$ in (15)).
(d) Utilize a state-space approach to model the internal hidden cognitive stress-related state, x_k in (1), to the changes in binarized neural impulses (9)-(12).
(e) Use the EM algorithm (4)-(5) to find the initial values (presented in Table 3) and estimate the cognitive stress-related state (i.e., $\hat{x}_k$, and its variance $\hat{\sigma}_k$).
(f) Analyze the estimated cognitive stress state and generating the environmental stimuli functions required for the real-time simulation system (i.e., s_k in (6)).

Real-time Closed-Loop System

(g) Incorporate the simulated environmental input, η_k, in (1), simulate the SCR events by assuming that they follow a Bernoulli distribution (i.e., n_k in (2)), and run the real-time system.
(h) Employ the Bayesian filtering approach (4)-(5) to track the internal cognitive stress state in real-time.
(i) Design the fuzzy control structure, including the rule base, membership functions, and inference engine for both inhibition and excitation purposes (i.e., Fig. 5 and Table 2).
(j) Implement the designed fuzzy controller and close the loop to regulate the estimated cognitive stress state.

III. RESULTS

Implementing the proposed WMI architecture on selected subjects' simulated profiles (Table 1), we present the results in this section. Particularly, we illustrate the results in three different cases: (A) open-loop cognitive stress tracking, (B) closed-loop inhibitory, and (C) closed-loop excitatory. For each case, we consider two environmental stimuli models in the simulation: (1) cognitive stress stimuli, and (2) relaxing stimuli. Following the offline process presented in Fig. 3, we simulate the environmental stimuli and run the simulation system in real-time. The final results are presented in Fig. 6-8. In each case, we consider the environmental stimuli associated with the high arousal (cognitive stress) and low arousal (relaxation period) in the first and second half of the simulation, respectively.

A. OPEN-LOOP

The main objective of presenting the open-loop case is to show how we could track the cognitive stress-related state without any control implemented (i.e., $u_k = 0$) in the developed simulation environment. As observed in the top sub-panels of Fig. 6, the number of SCR events significantly decreased in the second half of the simulation (i.e., relaxation period) because of the decreased sympathetic firing rate compared to the first half of the simulation (i.e., cognitive stress task). This variation in the number of SCR events results in a lower level of the estimated cognitive stress-related state (bottom sub-panels) in the relaxation period compared to the high arousal (cognitive stress) period. This open-loop case shows that our proposed algorithm is successful in tracking internal cognitive stress state in the real-time simulation environment.

B. CLOSED-LOOP INHIBITORY

In this case, we examine the performance of the proposed WMI architecture in lowering high levels of cognitive stress-related state caused by an high arousal environmental stimuli. By detecting high levels of cognitive stress state, the control systems attempts to regulate it in real-time. As presented in Fig. 7, the high number of SCR events and the higher levels of estimated cognitive stress-related state (top and middle sub-panels) are detected by the system and control becomes active (bottom sub-panel). Then, employing the derived control actions results in fewer number of SCR events and a lower levels of estimated stress state in the first half of the simulation (i.e., cognitive stress period). This closed-loop inhibitory case validates the performance of proposed WMI architecture in lowering the estimated cognitive stress-related state levels in a real-time manner.

C. CLOSED-LOOP EXCITATORY

As discussed earlier, it is important to keep one's cognitive stress levels within a desired range. Meaning, the cognitive stress state is sometimes considered as the cognitive engagement which is a positive stress (or eustress). Our goal in this case is to prevent cognitive disengagement. More particularly, as observed in Fig. 8, the small number of SCR events and the lower levels of estimated cognitive stress-related state (top and middle sub-panels) in the second half of the simulation (i.e., low cognitive engagement period) are detected by the

This article has been accepted for publication in a future issue of this journal, but has not been fully edited. Content may change prior to final publication. Citation information: DOI 10.1109/ACCESS.2021.3099027, IEEE Access

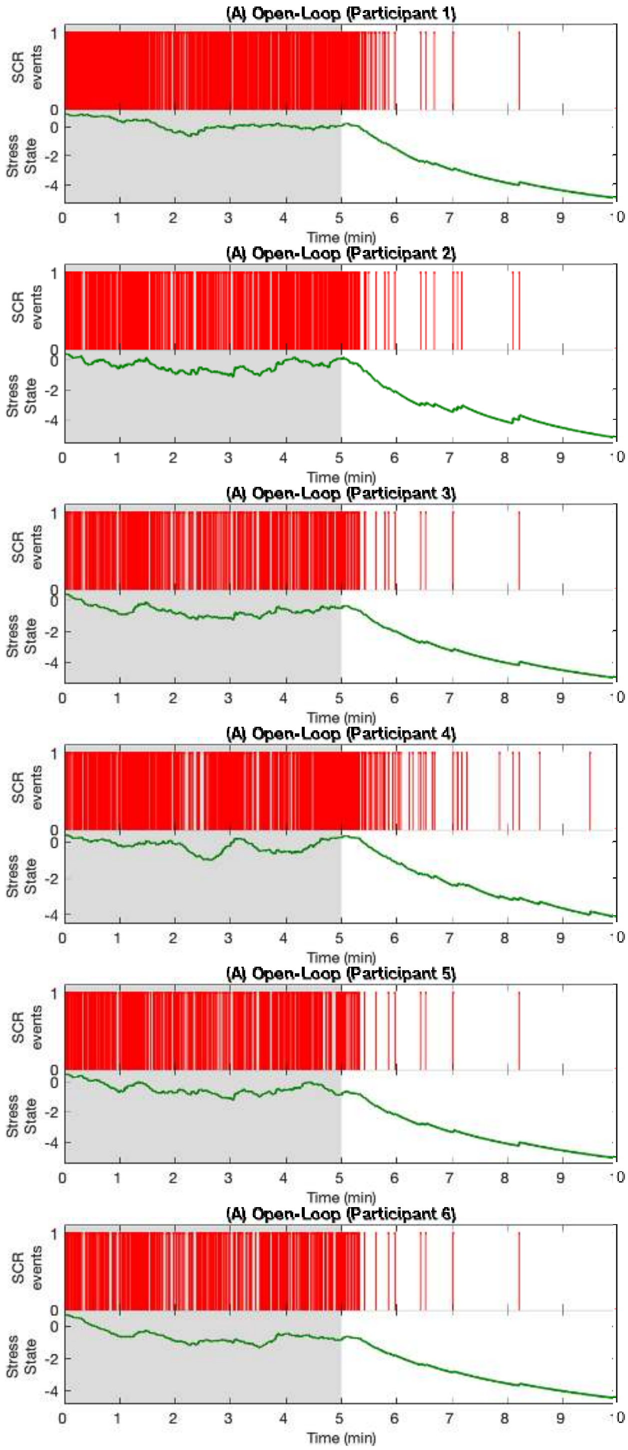

FIGURE 6. Open-loop results in WMI architecture. For each participant, the top sub-panel shows the SCR events from the human model, the bottom sub-panel displays the estimated cognitive stress-related state. The grey background belongs to the high arousal environmental stimuli (i.e., the cognitive stress task), while the white background implies the low arousal environmental stimuli (i.e., the relaxation task).

system. Then, employing the control signals (bottom sub-panel) results in more SCR events and a higher estimated cognitive-related state levels in this period of low cognitive

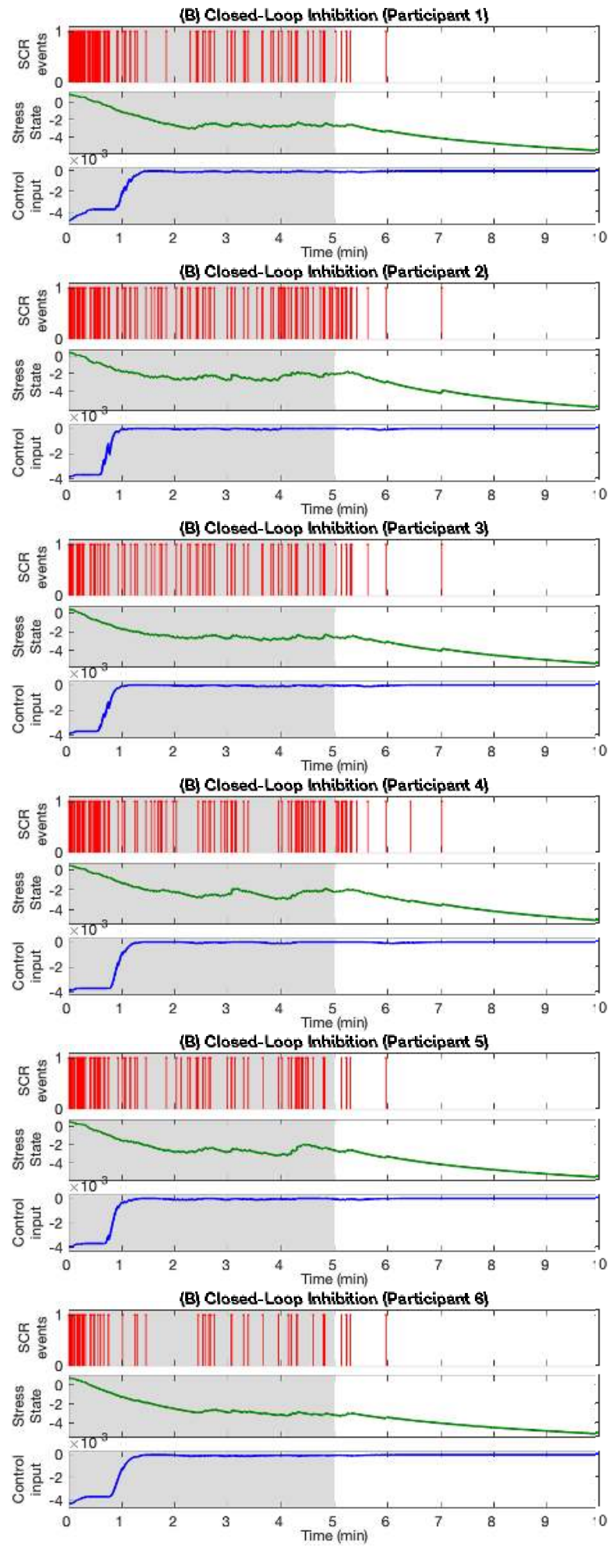

FIGURE 7. Closed-loop inhibition results in WMI architecture. For each participant, the top sub-panel shows the SCR events from the human model, the middle sub-panel displays the estimated cognitive stress-related state, and the bottom sub-panel depicts the control signal. The grey background belongs to the high arousal environmental stimuli (i.e., the cognitive stress task), while the white background implies the low arousal environmental stimuli (i.e., the relaxation task).

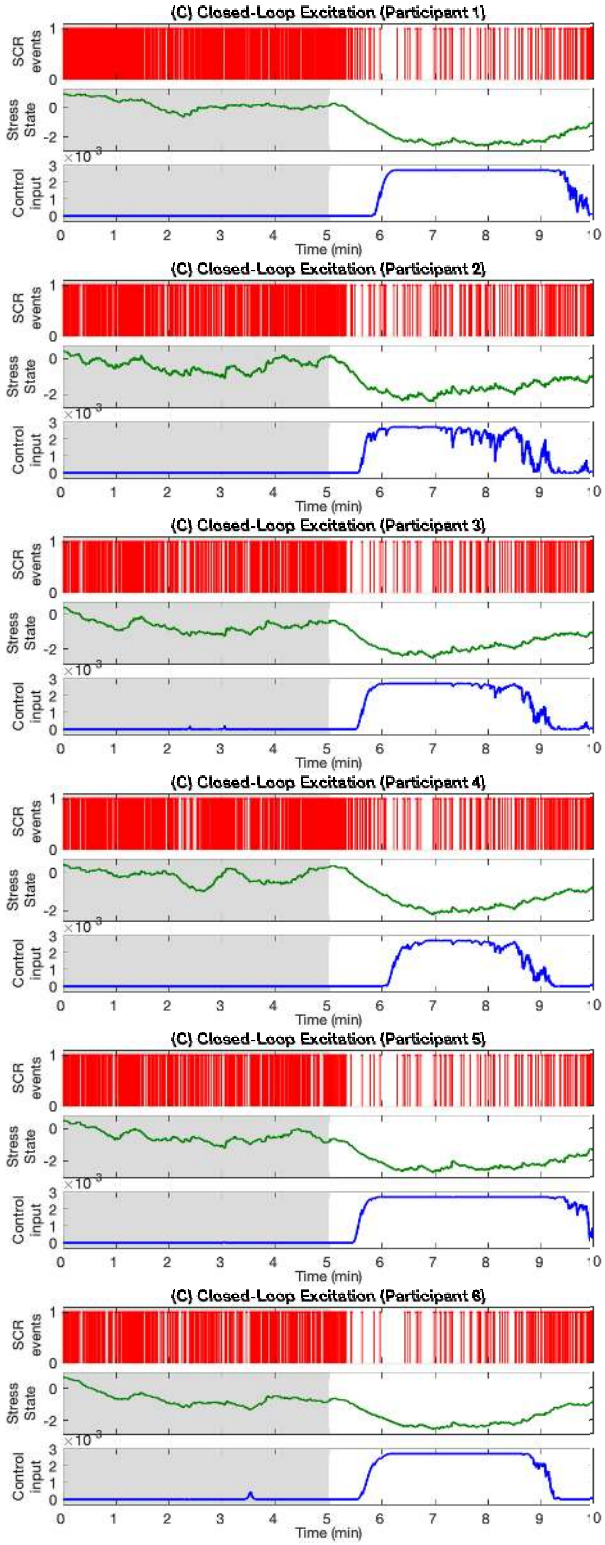

FIGURE 8. Closed-loop excitation results in WMI architecture. For each participant, the top sub-panel shows the SCR events from the human model, the middle sub-panel displays the estimated cognitive stress-related state, and the bottom sub-panel depicts the control signal. The grey background belongs to the high arousal environmental stimuli (i.e., the cognitive stress task), while the white background implies the low arousal environmental stimuli (i.e., the relaxation task).

engagement. This closed-loop excitatory case illustrates how the proposed WMI approach is effective in elevating the cognitive stress-related state in a real-time manner.

IV. DISCUSSION AND CONCLUSION

To design a simulation system for tracking and control internal cognitive stress state based on SCR events, we analyzed recorded data from multiple subjects in an offline process (Fig. 3). Next, we presented two different models for environmental stimuli: one for cognitive stress (high arousal) and one for relaxation (low arousal). Taking advantage of simulated environmental stimuli, we designed the real-time system for further analysis. By modeling SCR events, we employed the state-space approach to relate the internal cognitive stress state to the changes in SCR events. Using Bayesian filtering, we estimated the hidden cognitive stress-related state in real-time. To close the loop and regulate the estimated stress state, we designed a fuzzy control system in the proposed WMI architecture.

To the best of our knowledge, this research is one of the very first to relate the cognitive stress state to the changes in SCR events and designing the control mechanism to close the loop in a real-time simulation system. In particular, we accomplished the task of closed-loop cognitive stress regulation in a simulation study based on experimental data. The final results verify that the proposed architecture has great potential to be implemented in a wrist-worn wearable device and used in daily life. To illustrate this idea, we presented three cases. In the first case (Fig. 6), open-loop results demonstrated how the proposed architecture is successful in tracking internal stress state in both high and low arousal periods.

In the second case (Fig. 7), we investigated the performance of the proposed approach in cognitive stress inhibition. Here, we assumed that the first half of the simulation (first 5 min in Fig. 7) is associated with the undesired cognitive stress, which is due to an unpleasant stressful environment. The goal of lowering the estimated cognitive stress state is achieved by detecting the high arousal levels and applying the appropriate control action in the real-time system. Hence, the number of SCR events and the estimated cognitive stress levels have significantly dropped in the first half of the simulation compared to the same period of time in the open-loop case (Fig. 6). Furthermore, since the main goal in this case was to inhibit cognitive stress-related state, and as the second half of the simulation is associated with the low arousal session, the control input goes to zero during this time span. The simulated human brain responses in the second half of the simulation, which is related to low arousal (relaxation) environment, is affected by the inhibitory control applied in the first half of the simulation. For example, in an experiment with a cognitive task followed by a relaxation task, if a subject listens to relaxing music during the cognitive stress task to decrease his/her stress levels, he/she will be even more calmed during the relaxation period compared to a subject who did not listen to relaxing music during the cognitive stress task. So, the more calmed response in the second half of the simulation is due to the applied inhibitory control in the first half of the simulation. In other words, for the closed-loop inhibition case, while we do not observe any control action during the second half of the simulation, the number of SCR events and estimated stress levels are lower in this period of simulation compared to the open-loop case.

The final case is related to the condition in which we assume the simulated subject is not cognitively engaged with the environment. Here, we aimed to increase the arousal state which is useful for concentration and productivity [4]. Implementing the proposed excitatory WMI architecture, the number of SCR events and the estimated cognitive stress-related state have been elevated remarkably in the second half of the simulation compared to the same period of time in the open-loop case (Fig. 6). As a result, the proposed approach could be used to detect this low arousal state and increase it in real-time. It should be pointed out that, since the objective in this case was to excite cognitive stress-related state, and as the first half of the simulation is associated with the high arousal environmental stimuli, the control input will remain zero during this time period. From medical perspective, modulating the levels of cognitive stress and increasing eustress are potentially beneficial in individuals with anxiety and depression. In particular, patients with traumatic brain injury who suffer from both disorders could benefit from increased eustress to enhance their engagement during rehabilitation treatments [74].

To illustrate the performance of our proposed closed-loop architecture, we perform the t-test analysis on all six participants' results. To this end, we analyze the performance of the proposed closed-loop system for both inhibitory and excitatory controllers (See Fig. 13). Hence, we investigate the results of implemented control system on both simulated SCR events and estimates stress levels. We compute the number of observed SCR events per minute in both open-loop and closed-loop sessions for both high and low arousal periods (i.e., five minutes in each case). Moreover, to examine the effect of proposed architecture on the estimated stress state, we averaged the values associated with the estimated stress state in both open-loop and closed-loop sessions. The results of performing the t-test analysis on all simulated profiles are depicted in Fig. 9.

The decrease in the number of SCR events and average levels of estimated stress state presented in left sub-panels of Fig. 9 are due to the implemented inhibitory control system. Conversely, the increase in the number of SCR events and average levels of estimated stress state observed in right sub-panels of Fig. 9 are because of applying excitatory control system. In each t-test analysis, the resultant p-values presented on top of the arrows confirm the efficiency of the proposed closed-loop architecture in both inhibitory and excitatory classes.

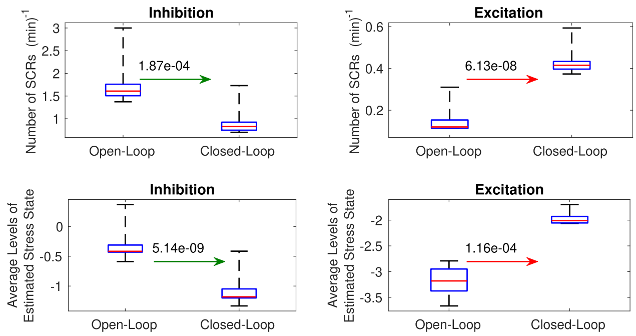

FIGURE 9. T-test performance analysis on all six participants. The left panels show the performance of the inhibitory closed-loop system. The right panels are associated with the results of the excitatory closed-loop system. The top panels depict the performance of the closed-loop system in regulating the number of SCR events per minute. The bottom panels show the performance of the closed-loop system in regulating the estimated stress levels. The numbers on top of the arrows stand for the corresponding p-values.

It should also be highlighted that different experimental environments would influence the results. In fact, this *in silico* study is based on the experiment in [12], in which the high and low arousal sessions are designed accordingly. In [12], the cognitive stress session is designed to ask the subjects to perform the Stroop and arithmetic tests, while the low arousal is derived by asking them to listen to relaxing music. While the performance of the proposed algorithm is validated by implementing it on multiple subjects' profiles, any changes in the reference experiment would further affect the subjects' skin conductance response and estimated stress state, accordingly.

In comparison to other available efforts that attempt to infer brain activity by directly monitoring it [11], [54], [75], [76], our proposed approach aims to detect the cognitive stress indirectly by collecting physiological signals from wearable devices and inferring the arousal state. Compared to the existing approaches, which classify the stress levels based on the physiological data and provide different classes of stress levels, the proposed approach tracks the stress state in a systematic way and in a continuous manner. The state-space model and Bayesian filter are in good agreement with the physiology underlying the sympathetic arousal activities [77], [78]. An increase in sympathetic arousal, which is a natural response to certain external stimuli, causes rise to measurable bio-signal such as skin conductance. The applied filter in this research takes the information presented in SCR changes and relates it to the hidden cognitive stress state.

Although scientists and engineers have performed research in the field of emotion regulation [49]–[51], [79]–[81], the present work is one of the first to present a simulation environment for designing closed-loop control algorithms based on the inferred arousal state. In the proposed architecture, the arousal decoder only requires a skin conductance signal that can be collected using wrist-worn wearable devices. Indeed, instead of using the raw skin conductance signal, we infer the underlying neural responses (i.e., the increase or decrease in sympathetic tone termed the skin conductance events rate) and use that information to decode the hidden arousal state. Then, we design the controller to close the loop. In this research, we demonstrated how the fuzzy control is successful in closing the loop and managing internal stress state. One of the main advantages of a fuzzy control structure is its expandability. This knowledge-based approach can be modified to cover different types of stress. The results on all simulated subjects' profiles verify the performance of the proposed architecture and show its feasibility to be implemented in the real world. Although the steps presented in section II-F provide the local stability condition in the proposed fuzzy controller in a finite time horizon window, it should be noted that finding the stability region in a closed form, and for an infinite time horizon, is not yet a tractable problem and needs further investigation [82]. Applying uncertainty-based control techniques is an alternative approach to establish a stable control system. While the proposed approach in this study employs point process analysis for state-space modeling and Bayesian filtering for the state estimation process, Li *et al.* proposed a novel adaptive fuzzy tracking and control system to handle the system nonlinearities both in the filter design and tracking procedures [83]. Another possible approach for closing the loop is to consider the model nonlinearities, which are present in the observations, while tracking the state and designing the control system [83].

In this *in silico* study, we made use of a publicly available dataset to create a virtual environment for real-time tracking and regulation of internal cognitive stress state. In what follows, we present some of the main challenges we faced in the design process. We used the skin conductance signal as a biomarker that carries valuable information about the autonomic nervous system and could be collected using wearable devices. Selecting clean profiles with fewer artifacts was one of the very first challenges addressed. Performing a deconvolution algorithm and Bayesian filtering to estimate the hidden cognitive stress-related state are the next important steps. To design the virtual environment, we successfully simulated environmental stimuli functions. This challenging step led us to evaluate the efficiency of the proposed architectures in stress tracking and closing the loop in real-time. The next challenging task is to design an appropriate control strategy for closing the loop and regulating the stress state. To this end, we employed fuzzy control as a powerful knowledge-based approach to enhance the closed-loop system with some expertise inference. Developing a unified fuzzy structure to efficiently regulate stress state in all simulated profiles is the next important step. By analyzing the open-loop results, we designed appropriate rule base, membership functions, and defuzzification method to ensure handling inter-subject variability in the proposed architecture and closed the loop.

The present research is the first attempt to design a virtual environment based on the experimental data and relate the internal cognitive stress state to the changes in skin conductance. Taking advantage of the developed system, we track cognitive stress state in real-time. By designing the control algorithm, we demonstrated the feasibility of the proposed closed-loop architectures to inhibit and excite the estimated stress state in real world.

V. CONCLUSION

The brain can be considered as a control system with a strong impact on all human functions, including health and performance. Inspired by recent advances in wearable technologies, we proposed a WMI architecture for controlling an internal cognitive stress state in a simulation environment. The WMI architecture encompasses collecting physiological data using wearable devices, inferring neural stimuli underlying pulsatile signals, estimating an unobserved state based on the underlying stimuli, designing the controller, and closing the loop in real-time. In this simulation work based on the experimental data, we followed the goal of designing a simulation environment by monitoring subjects' skin conductance variations (as a validated stress indicator). In the developed simulation system, we designed a fuzzy control system to close the loop and regulate the estimated cognitive stress-related state in real-time. The final results validate the performance of our proposed WMI architectures in accomplishing the tasks of (1) tracking the cognitive stress state, (2) lowering the levels of cognitive stress-related state by applying inhibitory control in high cognitive stress environments, and (3) elevating the cognitive stress-related state levels by applying excitatory control in low cognitive stress environments. All of these tasks are accomplished in an automatic closed-loop manner. The present work is an important first step which will ultimately lead to help patients suffering from stress and anxiety disorders.

VI. FUTURE DIRECTIONS

One future application of the proposed architecture could be incorporating potential non-invasive actuation effective in regulating arousal state in the real-life human-in-the-loop scenarios. The examples of these actuation are listening to music [84]–[87], adjusting the light in workplaces [88]–[90], smelling fragrances [91]–[93], and drinking beverages such as coffee, tea, and water [94]. Using different actuators and wearable devices, one may perform system identification and model the actuation dynamics [95]–[99]. Considering subject-specific reactions and possible latency in skin conductance responses to any actuation [100], one may model the actuation dynamics and include them in the experimental WMI architectures. In such practical WMI architectures, a wearable device measures related bio-signal skin conductance signal (instead of environmental stimuli function presented in Fig. 3 (B) that is required for the real-time simulation analysis), a decoder estimates the cognitive stress state, and a controller brings the cognitive stress to the desired range by incorporating modeled non-invasive actuation in a closed-loop manner.

Since the skin conductance can also be varied in response to other types of stimuli, analyzing valence variation could be

This article has been accepted for publication in a future issue of this journal, but has not been fully edited. Content may change prior to final publication. Citation information: DOI 10.1109/ACCESS.2021.3099027, IEEE Access

another future direction of this research. By analyzing more physiological measurements, we might be able to differentiate between excitement and nervousness as well. Moreover, as SCR events are assumed to follow a Bernoulli distribution, we did not include measurement noise in the filter design. In the future experimental WMI architecture, measurement noise should be incorporated for inferring SCR events. While the current fuzzy control system is designed in a simple single-input single-output structure, it has the capability to be further expanded and incorporates multiple physiological measurements from wearable device(s). Accordingly, the expanded multi-input multi-output system would be designed in a way to take data from multiple sources, performs appropriate analysis, and governs the control action to regulate corresponding internal states. Furthermore, investigating more advanced control approaches such as genetic algorithm on top of fuzzy structure [101] might enable us to optimize the actuation design and achieve the ultimate goal of practically employing the WMI architectures to manage individuals' internal states.

APPENDIX A
DECONVOLUTION

In the offline process, as it is described in the methods section, we need to perform a deconvolution algorithm to infer underlying neural stimuli. While we have followed the approaches presented in [21], [26], in what follows we present a brief description of the deconvolution method.

Skin conductance signal $y_{SC}(t)$ contains two parts; tonic and phasic parts [21], [26]. The tonic which is slow varying in nature is highly related to thermoregulation and is a function of ambient temperature and humidity. The phasic part which includes faster changes is generated by sympathetic nerve fibers stimulating the sweat glands:

$$y_{SC}(t) = y_P(t) + y_T(t), \tag{8}$$

where $y_P(t)$ and $y_T(t)$ stand for the phasic and tonic components, respectively. The phasic part $y_P(t)$ is extracted from the skin conductance signal by an algorithm such as cvxEDA [73]. The physiology behind the formation of the phasic component could be found in detail in [21], [26], [65], [102], [103] and will result in the following state-space model:

$$\dot{z}_1(t) = -\frac{1}{\theta_r} z_1(t) + \frac{1}{\theta_r} u(t) \qquad \text{(diffusion)}, \tag{9}$$

$$\dot{z}_2(t) = \frac{1}{\theta_d} z_1(t) - \frac{1}{\theta_d} z_2(t) \qquad \text{(evaporation)}. \tag{10}$$

where $z_1(t)$ and $z_2(t)$ are internal state and the phasic component, respectively. $u(t)$ represents the neural stimuli to the sweat glands to cause skin conductance responses (SCR). θ_r and θ_d are the rise and decay times of a single SCR. As the number of underlying neural impulses, which causing the SCRs, is also small, it leads us to employ a sparsity constraint when solving for $u(t)$. We model $u(t)$ as a finite summation

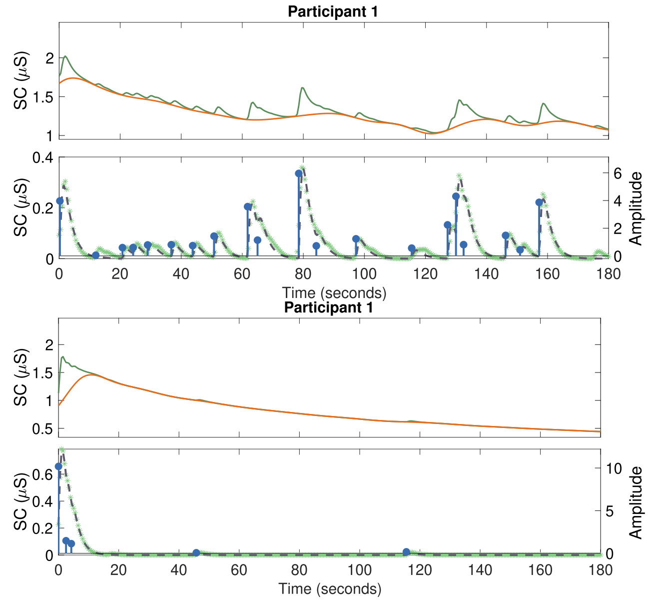

FIGURE 10. **Experimental skin conductance signals along with deconvolution results [26]. Upper panel shows the results associated with the high arousal (cognitive stress), and the bottom panel displays the results corresponding to the low arousal (relaxation). In each panel, the top sub-panel shows the raw skin conductance data (green curve) and its extracted tonic component using cvxEDA (orange curve); the bottom sub-panel depicts the extracted phasic component (green stars), the estimated reconstructed signal (dashed black curve), the estimated SCR events (blue vertical lines).**

of weighted, shifted delta functions:

$$u(t) = \sum_{i=1}^{N} u_i \delta(t - \Delta_i), \tag{11}$$

where u_i represents the SCR's amplitude at time Δ_i, and N is the total number of samples in the neural stimuli signal and is proportional to the recording duration T_d and the input sampling frequency f_u ($N = T_d \cdot f_u$). We consider the phasic part $z_2(t)$ as the output in the state-space model:

$$y_P(t) = z_2(t) + \mu(t). \tag{12}$$

where $\mu(t)$ is Gaussian measurement noise. If the signal is periodically sampled at T_y intervals to yield a total of M measurements, we can define the equivalent discrete-time observation y_k as:

$$y_k = x_2(kT_y) + \mu_k. \tag{13}$$

Given all the discrete measurements $y_k = y_P(k)$ for $k = 1, 2, \ldots, M$, we aim to find $u(t)$ and estimate θ_r and θ_d. We take $z_1(0) = 0$ as an initial condition assuming that the sweat duct is empty at the beginning. The state-space solution for $z_2(kT_y)$ leads us to [24]:

$$y_k = a_k y_0 + \mathbf{b}_k \mathbf{u} + \mu_k, \tag{14}$$

where $a_k = e^{-\frac{kT_y}{\theta_d}}$, $\mathbf{b}_k = \big[\frac{1}{(\theta_r-\theta_d)}(e^{-\frac{kT_y}{\theta_r}} - e^{-\frac{kT_y}{\theta_d}})$ $\frac{1}{(\theta_r-\theta_d)}(e^{-\frac{kT_y-T_u}{\theta_r}} - e^{-\frac{kT_y-T_u}{\theta_d}})$ $\frac{1}{(\theta_r-\tau_d)}(e^{-\frac{kT_y-2T_u}{\theta_r}} - e^{-\frac{kT_y-2T_u}{\theta_d}})$

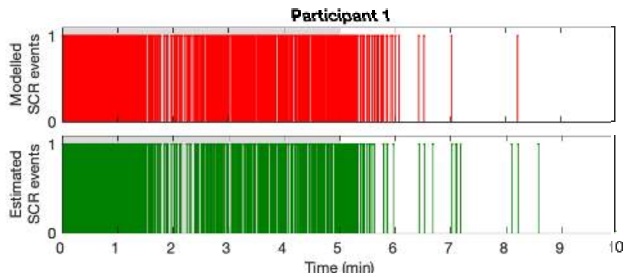

FIGURE 11. Adequacy of SCR events. The top sub-panel shows the modeled SCR events from the human model, and the bottom sub-panel displays the estimated SCR events. The grey background belongs to the high arousal environmental stimuli (i.e., the cognitive stress task) and the white background implies the low arousal environmental stimuli (i.e., the relaxation task).

TABLE 3. EM algorithm initialization.

Participant	Reference session	x_0	σ_0^2
1	High arousal	0.9134	0.00049
	Low arousal	0.8312	0.00032
	Combined sessions	0.8817	0.00041
2	High arousal	0.4473	0.00087
	Low arousal	0.3501	0.00071
	Combined sessions	0.4112	0.00080
3	High arousal	0.4334	0.00047
	Low arousal	0.3815	0.00032
	Combined sessions	0.4209	0.00041
4	High arousal	0.4501	0.00036
	Low arousal	0.3318	0.00024
	Combined sessions	0.4017	0.00031
5	High arousal	0.5333	0.00044
	Low arousal	0.4321	0.00039
	Combined sessions	0.4983	0.00042
6	High arousal	0.7434	0.00022
	Low arousal	0.7102	0.00015
	Combined sessions	0.7321	0.00019

$\cdots \quad \frac{1}{(\theta_r-\theta_d)}(e^{-\frac{T_u}{\theta_r}} - e^{-\frac{T_u}{\theta_d}}) \quad \underbrace{0 \quad \cdots \quad 0}_{N-\frac{kT_y}{T_u}}]$, and $\mathbf{u} = [u_1 \quad u_2 \quad \cdots \quad u_N]^\top$ represents a sparse vector containing all the neural stimuli over the entire signal duration (i.e., very few of the u_i's are non-zero). Concatenating all the measurements into a single vector $\mathbf{y} = [y_1 \quad y_2 \quad \cdots \quad y_M]^\top$ we derive,

$$\mathbf{y} = \mathbf{A}_\theta y_0 + \mathbf{B}_\theta \mathbf{u} + \boldsymbol{\mu}, \tag{15}$$

where $\mathbf{A}_\theta = [a_1 \quad a_2 \quad \cdots \quad a_M]^\top$, $\mathbf{B}_\theta = [\mathbf{b}_1^\top \quad \mathbf{b}_2^\top \quad \cdots \quad \mathbf{b}_M^\top]^\top$, $\boldsymbol{\mu} = [\mu_1 \quad \mu_2 \quad \cdots \quad \mu_M]^\top$, and y_0 is the initial condition of the phasic skin conductance signal. Here, T_y is an integer multiple of T_u. Letting $\boldsymbol{\theta} = [\theta_r \quad \theta_d]^\top$, to derive the SCR events $\mathbf{u}$, we aim to solve the following optimization problem:

$$\underset{\substack{\boldsymbol{\theta},\,\mathbf{u} \\ C\boldsymbol{\theta}\leq b,\ \mathbf{u}\geq 0}}{\text{argmin}} \quad J(\boldsymbol{\theta}, \mathbf{u}) = \frac{1}{2}||\mathbf{y} - \mathbf{A}_\theta y_0 - \mathbf{B}_\theta \mathbf{u}||_2^2 + \lambda||\mathbf{u}||_p^p, \tag{16}$$

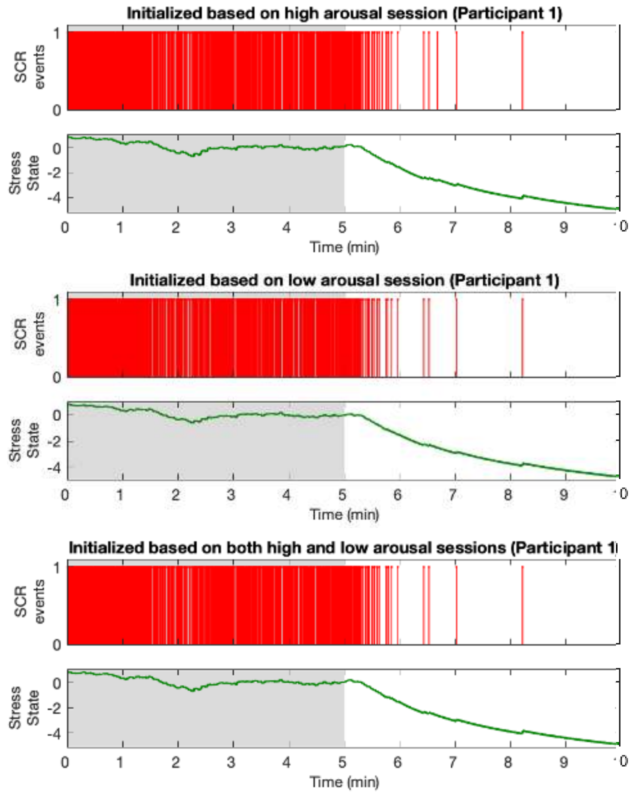

FIGURE 12. Open-loop results based on different EM initialization. The top panel shows the results while the filter is initialized based on the high arousal session. The middle panel shows the results while the filter is initialized based on the low arousal session. The bottom panel shows the results while the filter is initialized using both high and low arousal sessions. In each panel, the top sub-panel displays the SCR events, while the bottom sub-panel displays the estimated cognitive stress-related state. The grey background belongs to the high arousal environmental stimuli (i.e., the cognitive stress task), while the white background implies the low arousal environmental stimuli (i.e., the relaxation task).

where $C = \begin{bmatrix} -1 & 1 & 0 & 0 \\ 0 & 0 & -1 & 1 \end{bmatrix}^\top$, $b = [-0.1 \quad 1.4 \quad -1.5 \quad 6]^\top$ and λ is the l_p-norm regularization parameter determining the sparsity level on $\mathbf{u}$. Due to the unavoidable challenges in solving this optimization problem, we follow the approaches presented in [24], [27], [36], [104] and break it into two sub-problems. A desired coordinate descent approach can be formulated as:

1) $\mathbf{u}^{(l+1)} = \underset{\substack{\mathbf{u} \\ \text{s.t.}\ \mathbf{u}\geq 0}}{\text{argmin}}\ J_\lambda(\boldsymbol{\theta}^{(l)}, \mathbf{u})$
2) $\boldsymbol{\theta}^{(l+1)} = \underset{\substack{\boldsymbol{\theta} \\ \text{s.t.}\ C\boldsymbol{\theta}\leq b}}{\text{argmin}}\ J(\boldsymbol{\theta}, \mathbf{u}^{(l+1)})$

To derive the final answer, we iteratively solve the above sub-problems (for $l = 0, 1, 2, \cdots$) until convergence. We present the results of performing the explained deconvolution algorithm in Fig. 10 [26]. Fig. 10 includes results associated with the skin conductance signals along with the deconvolution results for the participant 1 during both the cognitive stress and the relaxation sessions in original experiment [12].

This article has been accepted for publication in a future issue of this journal, but has not been fully edited. Content may change prior to final publication. Citation information: DOI 10.1109/ACCESS.2021.3099027, IEEE Access

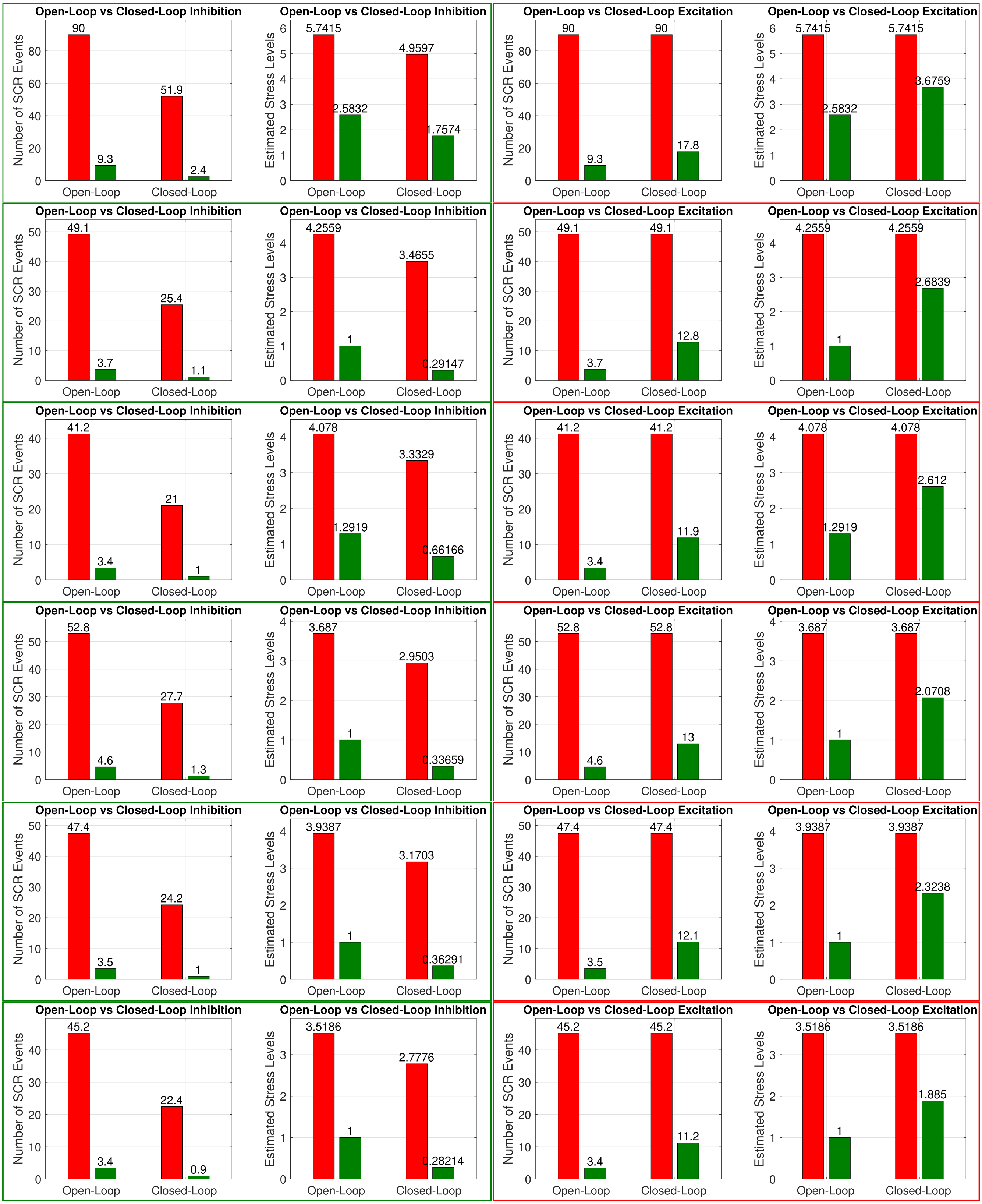

FIGURE 13. **Closed-loop performance evaluation for all participants. Each row of sub-plots belongs to one participant. In each row, left green and right red panels show the performance of inhibitory and excitatory class of closed-loop systems, respectively. In each panel, while the left one is associated with the total number of SCR events, the right one is related to the average levels of estimated cognitive stress state. Red bars are related to the first half of the experiment (i.e., high arousal session) and green bars are related to the second half of the simulation (i.e., low arousal session). In order to better present the results, the subject's baseline has been deducted from the averaged estimated stress state levels.**

Wickramasuriya *et al.* analyzed the accuracy of proposed deconvolution algorithm by implementing it on a second set of synthetic data [26]. In [26], they added a 25 dB SNR Gaussian noise to corrupt the simulated phasic skin conductance signal. The results presented in [26] demonstrate that the proposed deconvolution algorithm could successfully recover the underlying neural impulses in the presence of measurement noises (Figure 3 and Table 2 in [26]).

APPENDIX B
SCR MODELING

To show the adequacy of SCR events modeled in the real-time system, we present both modeled and estimated SCR events for participant 1 in Fig. 11. We presented the results in open-loop case without applying control input ($u_k = 0$). In Fig. 11, the top sub-panel and the bottom sub-panel show the modeled SCR events and estimated SCR events, respectively.

APPENDIX C
EM ALGORITHM INITIALIZATION

As presented in Fig. 3, and discussed in part II-C, we perform EM algorithm to estimate the initial values (i.e., x_0 and σ_0^2) [26], [59], [66]. This step is important in designing the real-time filter to estimate the state. Hence, we estimate these initial values in three different scenarios and compare the outcome. We derive the initial values using EM algorithm employing: (1) high arousal session, (2) low arousal session, and (3) combined sessions. The resulted initial values are presented in Table 3. To analyze the system performance in response to these different initializations, we present the open-loop results for participant 1 in Fig. 12.

As presented in Fig. 12, different initial values, which are derived based on different sessions, do not significantly affect the state estimation performance. The open-loop results presented in Fig. 12 verify that the implemented Bayesian filter is sufficiently robust to the offline EM initialization process.

APPENDIX D
CLOSED-LOOP ANALYSIS

To further analyze the performance of the closed-loop system, we present the following Fig. 13 on achieved results. Analyzing the final results on all simulated subjects, we present the effect of the real-time closed-loop system in decreasing (increasing) the number of SCR events and lowering (elevating) the levels of estimated stress state in Fig. 13. As depicted in Fig. 13, each row belongs to one subject. In each row, left panel (big green box) and right panel (big red box) are related to the inhibitory and excitatory closed-loop cases, respectively. In each colored box, the left sub-panel is related to the total number of observed SCR events in each high/low arousal session, while the right sub-panel depicts the difference in the average levels of stress state in each session. Red bars are associated with the first half of the simulation (i.e., high arousal or cognitive stress period), while the green bars are related to the second half of the simulation (i.e., low arousal or relaxation period). In what follows, we explain the results presented in Fig. 13.

By running the closed-loop system and observing the results, we analyze the performance of the proposed closed-loop system for both inhibitory (big green box in each row) and excitatory (big red box in each row) controllers. To better show the performance, we present the results of the implemented control system on both simulated SCR events (left sub-panels) and estimated stress levels (right sub-panels). In both closed-loop cases, we summed the number of SCR events in both high arousal (red bars) and low arousal (green bars) periods of the simulations. To analyze the performance of the closed-loop system on the estimated stress levels, we averaged the levels of estimated stress state over both high arousal (red bars) and low arousal (green bars) sessions (right sub-panels).

The decline in the total number of SCR events and the average levels of estimated stress state in the first half of the simulation (red bars) is due to the applied inhibitory controller in the high arousal session. Similarly, the increase in the total number of SCR events and the average levels of estimated stress state in the second half of the simulation (green bars) is due to the applied excitatory controller in the low arousal session.

ACKNOWLEDGMENT

This article was presented in part at the proceedings of the IEEE Engineering in Medicine and Biology Society Conference [1].

REFERENCES

[1] H. F. Azgomi, D. S. Wickramasuriya, and R. T. Faghih, "State-space modeling and fuzzy feedback control of cognitive stress," in *Proc. 41st Annu. Int. Conf. IEEE Eng. Med. Biol. Soc. (EMBC)*, Jul. 2019, pp. 6327–6330.

[2] R. J. McNally, D. J. Robinaugh, G. W. Y. Wu, L. Wang, M. K. Deserno, and D. Borsboom, "Mental disorders as causal systems: A network approach to posttraumatic stress disorder," *Clin. Psychol. Sci.*, vol. 3, no. 6, pp. 836–849, Nov. 2015.

[3] J. Thom, J. Bretschneider, N. Kraus, J. Handerer, and F. Jacobi, "Healthcare epidemiology of mental disorders: Why is the prevalence not declining despite growing provision of care?" *Bundesgesundheitsblatt, Gesundheitsforschung, Gesundheitsschutz*, vol. 62, no. 2, pp. 128–139, 2019.

[4] C. Gibbons, M. Dempster, and M. Moutray, "Stress and eustress in nursing students," *J. Adv. Nursing*, vol. 61, no. 3, pp. 282–290, Jan. 2008.

[5] E. Niki, "Oxidative stress and antioxidants: Distress or eustress?" *Arch. Biochemistry Biophys.*, vol. 595, pp. 19–24, Apr. 2016.

[6] A. J. Tomiyama, "Stress and obesity," *Annu. Rev. Psychol.*, vol. 70, pp. 703–718, Jan. 2019.

[7] R. K. Pradeep, "Stress management of women managers a comparative study of public sector and private sector banks in Kerala," Ph.D. dissertation, Dept. Commerce, Kuriakose Gregorios College, Mahatma Gandhi Univ., Kottayam, India, 2016.

[8] F. Pallavicini, L. Argenton, N. Toniazzi, L. Aceti, and F. Mantovani, "Virtual reality applications for stress management training in the military," *Aerosp. Med. Human Perform.*, vol. 87, no. 12, pp. 1021–1030, Dec. 2016.

[9] A. Bougea, N. Spantideas, and G. P. Chrousos, "Stress management for headaches in children and adolescents: A review and practical recommendations for health promotion programs and well-being," *J. Child Health Care*, vol. 22, no. 1, pp. 19–33, Mar. 2018.

[10] D. S. Wickramasuriya and R. T. Faghih, "A cortisol-based energy decoder for investigation of fatigue in hypercortisolism," in *Proc. 41st Annu. Int. Conf. IEEE Eng. Med. Biol. Soc. (EMBC)*, Jul. 2019, pp. 11–14.

[11] F. Al-Shargie, T. B. Tang, N. Badruddin, and M. Kiguchi, "Mental stress quantification using eeg signals," in *Proc. Int. Conf. Innov. Biomed. Eng. Life Sci.* Singapore: Springer, 2015, pp. 15–19.

[12] J. Birjandtalab, D. Cogan, M. B. Pouyan, and M. Nourani, "A non-EEG biosignals dataset for assessment and visualization of neurological status," in *Proc. IEEE Int. Workshop Signal Process. Syst. (SiPS)*, Oct. 2016, pp. 110–114.

[13] S.-S. Lin, C.-W. Lan, H.-Y. Hsu, and S.-T. Chen, "Data analytics of a wearable device for heat stroke detection," *Sensors*, vol. 18, no. 12, p. 4347, Dec. 2018.

[14] Y. S. Can, B. Arnrich, and C. Ersoy, "Stress detection in daily life scenarios using smart phones and wearable sensors: A survey," *J. Biomed. Informat.*, vol. 92, Apr. 2019, Art. no. 103139.

[15] S. Majumder, T. Mondal, and M. J. Deen, "Wearable sensors for remote health monitoring," *Sensors*, vol. 17, no. 1, p. 130, 2017.

[16] A. Sano and R. W. Picard, "Stress recognition using wearable sensors and mobile phones," in *Proc. Humaine Assoc. Conf. Affect. Comput. Intell. Interact.*, Sep. 2013, pp. 671–676.

[17] M. R. Amin and R. T. Faghih, "Robust inference of autonomic nervous system activation using skin conductance measurements: A multichannel sparse system identification approach," *IEEE Access*, vol. 7, pp. 173419–173437, 2019.

[18] M. R. Amin and R. T. Faghih, "Inferring autonomic nervous system stimulation from hand and foot skin conductance measurements," in *Proc. 52nd Asilomar Conf. Signals, Syst., Comput.*, Oct. 2018, pp. 655–660.

[19] B. Byrom, M. McCarthy, P. Schueler, and W. Muehlhausen, "Brain monitoring devices in neuroscience clinical research: The potential of remote monitoring using sensors, wearables, and mobile devices," *Clin. Pharmacol. Therapeutics*, vol. 104, no. 1, pp. 59–71, Jul. 2018.

[20] V. Jha, N. Prakash, and S. Sagar, "Wearable anger-monitoring system," *ICT Exp.*, vol. 4, no. 4, pp. 194–198, Dec. 2018.

[21] M. R. Amin and R. T. Faghih, "Sparse deconvolution of electrodermal activity via continuous-time system identification," *IEEE Trans. Biomed. Eng.*, vol. 66, no. 9, pp. 2585–2595, Sep. 2019.

[22] H. Thapliyal, V. Khalus, and C. Labrado, "Stress detection and management: A survey of wearable smart health devices," *IEEE Consum. Electron. Mag.*, vol. 6, no. 4, pp. 64–69, Oct. 2017.

[23] C. Setz, B. Arnrich, J. Schumm, R. L. Marca, G. Tröster, and U. Ehlert, "Discriminating stress from cognitive load using a wearable EDA device," *IEEE Trans. Inf. Technol. Biomed.*, vol. 14, no. 2, pp. 410–417, Mar. 2010.

[24] R. T. Faghih, P. A. Stokes, M.-F. Marin, R. G. Zsido, S. Zorowitz, B. L. Rosenbaum, H. Song, M. R. Milad, D. D. Dougherty, E. N. Eskandar, A. S. Widge, E. N. Brown, and R. Barbieri, "Characterization of fear conditioning and fear extinction by analysis of electrodermal activity," in *Proc. 37th Annu. Int. Conf. IEEE Eng. Med. Biol. Soc. (EMBC)*, Aug. 2015, pp. 7814–7818.

[25] X. Deng, R. T. Faghih, R. Barbieri, A. C. Paulk, W. F. Asaad, E. N. Brown, D. D. Dougherty, A. S. Widge, E. N. Eskandar, and U. T. Eden, "Estimating a dynamic state to relate neural spiking activity to behavioral signals during cognitive tasks," in *Proc. 37th Annu. Int. Conf. IEEE Eng. Med. Biol. Soc. (EMBC)*, Aug. 2015, pp. 7808–7813.

[26] D. S. Wickramasuriya, M. R. Amin, and R. T. Faghih, "Skin conductance as a viable alternative for closing the deep brain stimulation loop in neuropsychiatric disorders," *Frontiers Neurosci.*, vol. 13, p. 780, Aug. 2019.

[27] D. S. Wickramasuriya, C. Qi, and R. T. Faghih, "A state-space approach for detecting stress from electrodermal activity," in *Proc. 40th Annu. Int. Conf. IEEE Eng. Med. Biol. Soc. (EMBC)*, Jul. 2018, pp. 3562–3567.

[28] M. R. Amin and R. T. Faghih, "Tonic and phasic decomposition of skin conductance data: A generalized-cross-validation-based block coordinate descent approach," in *Proc. 41st Annu. Int. Conf. IEEE Eng. Med. Biol. Soc. (EMBC)*, Jul. 2019, pp. 745–749.

[29] H. D. Critchley, "Electrodermal responses: What happens in the brain," *Neuroscientist*, vol. 8, no. 2, pp. 132–142, 2002.

[30] H. F. Posada-Quintero, J. P. Florian, A. D. Orjuela-Cañón, and K. H. Chon, "Electrodermal activity is sensitive to cognitive stress under water," *Frontiers Physiol.*, vol. 8, p. 1128, Jan. 2018.

[31] A. Liapis, C. Katsanos, D. Sotiropoulos, M. Xenos, and N. Karousos, "Recognizing emotions in human computer interaction: Studying stress using skin conductance," in *Proc. Int. Conf. Hum.-Comput. Interact.* Bamberg, Germany: Springer, 2015, pp. 255–262.

[32] M. Mestanlk, Z. Vlsnovcova, and I. Tonhajzerova, "The assessment of the autonomic response to acute stress using electrodermal activity," *Acta Medica Martiniana*, vol. 14, no. 2, pp. 5–9, Sep. 2014.

[33] D. J. Clark, S. A. Chatterjee, T. E. McGuirk, E. C. Porges, E. J. Fox, and C. K. Balasubramanian, "Sympathetic nervous system activity measured by skin conductance quantifies the challenge of walking adaptability tasks after stroke," *Gait Posture*, vol. 60, pp. 148–153, Feb. 2018.

[34] M. E. Dawson, A. M. Schell, and D. L. Filion, "The electrodermal system," in *Handbook of Psychophysiology*. Cambridge, U.K.: Cambridge Univ. Press, 2017, pp. 217–243.

[35] Y. Ohtaki, A. Suzuki, and G. Papastefanou, "Integration of psychophysiological and behavioral indicators with ambulatory tracking for momentary indoor activity assessment," in *Proc. ICCAS-SICE*, 2009, pp. 499–502.

[36] R. T. Faghih, "From physiological signals to pulsatile dynamics: A sparse system identification approach," in *Dynamic Neuroscience*. Cham, Switzerland: Springer, 2018, pp. 239–265.

[37] H. Silva, A. Fred, and A. Lourenço, "Electrodermal response propagation time as a potential psychophysiological marker," in *Proc. Annu. Int. Conf. IEEE Eng. Med. Biol. Soc.*, Aug. 2012, pp. 6756–6759.

[38] A. Vartak, C. Fidopiastis, D. Nicholson, and W. Mikhael, "Estimation of arousal using decomposed skin conductance features-biomed 2009," *Biomed. Sci. Instrum.*, vol. 45, pp. 77–82, Jan. 2009.

[39] J. D. Isen, W. G. Iacono, and S. M. Malone, "Characterizing electrodermal response habituation: A latent class approach with application to psychopathology," *Psychophysiology*, vol. 50, no. 10, pp. 954–962, 2013.

[40] B.-G. Lee and W.-Y. Chung, "Wearable glove-type driver stress detection using a motion sensor," *IEEE Trans. Intell. Transp. Syst.*, vol. 18, no. 7, pp. 1835–1844, Jul. 2017.

[41] T. S. Perry, "Wearable sensor detects stress in sweat: Cortisol is key to tracking stress, but it's tough to measure in an instant—[News]," *IEEE Spectr.*, vol. 55, no. 9, pp. 14–15, Sep. 2018.

[42] F. Lebepe, G. Niezen, G. P. Hancke, and T. D. Ramotsoela, "Wearable stress monitoring system using multiple sensors," in *Proc. IEEE 14th Int. Conf. Ind. Informat. (INDIN)*, Jul. 2016, pp. 895–898.

[43] N. Tateyama, K. Ueda, and M. Nakao, "Development of an active sensing system for distress detection using skin conductance response," in *Proc. 8th Int. Conf. Affect. Comput. Intell. Interact. (ACII)*, Sep. 2019, pp. 1–6.

[44] L. Rachakonda, P. Sundaravadivel, S. P. Mohanty, E. Kougianos, and M. Ganapathiraju, "A smart sensor in the IoMT for stress level detection," in *Proc. IEEE Int. Symp. Smart Electron. Syst. (iSES) (Formerly iNiS)*, Dec. 2018, pp. 141–145.

[45] Y. S. Can, N. Chalabianloo, D. Ekiz, and C. Ersoy, "Continuous stress detection using wearable sensors in real life: Algorithmic programming contest case study," *Sensors*, vol. 19, no. 8, p. 1849, Apr. 2019.

[46] T. Panure and S. Sonawani, "Novel approach for stress detection using smartphone and E4 device," in *Proc. Int. Conf. Sustain. Commun. Netw. Appl.* Erode, India: Springer, 2019, pp. 736–745.

[47] M. Choi, G. Koo, M. Seo, and S. W. Kim, "Wearable device-based system to monitor a driver's stress, fatigue, and drowsiness," *IEEE Trans. Instrum. Meas.*, vol. 67, no. 3, pp. 634–645, Mar. 2018.

[48] V. Branson, D. Turnbull, M. J. Dry, and E. Palmer, "How do young people experience stress? A qualitative investigation of the indicators of distress and eustress in adolescents," *Int. J. Stress Manage.*, 2019. [Online]. Available: https://doi.apa.org/doiLanding?doi=10.1037%2Fstr0000102

[49] K. McKee, M. Russell, J. Mennis, M. Mason, and M. Neale, "Emotion regulation dynamics predict substance use in high-risk adolescents," *Addictive Behav.*, vol. 106, Jul. 2020, Art. no. 106374.

[50] Z.-H. Wang, Y. Wang, B.-Q. Liu, D.-N. Pan, and X. Li, "Neurological foundations of the brain in the automatic emotion regulation of anger and fear," in *Proc. IEEE 17th Int. Conf. Cognit. Informat. Cognit. Comput. (ICCI CC)*, Jul. 2018, pp. 228–233.

[51] P. A. Nogueira, R. Rodrigues, E. Oliveira, and L. E. Nacke, "Guided emotional state regulation: Understanding and shaping players's affective experiences in digital games," in *Proc. 9th Artif. Intell. Interact. Digit. Entertainment Conf.*, 2013, pp. 1–7.

[52] J.-X. Zhang and G.-H. Yang, "Robust adaptive fault-tolerant control for a class of unknown nonlinear systems," *IEEE Trans. Ind. Electron.*, vol. 64, no. 1, pp. 585–594, Jan. 2017.

[53] X. Zhang and Y. Chen, "Admissibility and robust stabilization of continuous linear singular fractional order systems with the fractional order α: The $0 < \alpha < 1$ case," *ISA Trans.*, vol. 82, pp. 42–50, Nov. 2018.

[54] C. B. Walter, "EEG workload prediction in a closed-loop learning environment," Ph.D. dissertation, Dept. Math. Natural Sci., Universität Tübingen, Tübingen, Germany, 2015.

[55] J.-X. Zhang and G.-H. Yang, "Prescribed performance fault-tolerant control of uncertain nonlinear systems with unknown control directions," *IEEE Trans. Autom. Control*, vol. 62, no. 12, pp. 6529–6535, Dec. 2017.

[56] H. F. Azgomi and J. Poshtan, "Induction motor stator fault detection via fuzzy logic," in *Proc. 21st Iranian Conf. Electr. Eng. (ICEE)*, May 2013, pp. 1–5.

[57] H. F. Azgomi, J. Poshtan, and M. Poshtan, "Experimental validation on stator fault detection via fuzzy logic," in *Proc. 3rd Int. Conf. Electr. Power Energy Convers. Syst.*, Oct. 2013, pp. 1–6.

[58] J.-X. Zhang and G.-H. Yang, "Fuzzy adaptive output feedback control of uncertain nonlinear systems with prescribed performance," *IEEE Trans. Cybern.*, vol. 48, no. 5, pp. 1342–1354, May 2018.

[59] A. C. Smith, L. M. Frank, S. Wirth, M. Yanike, D. Hu, Y. Kubota, A. M. Graybiel, W. A. Suzuki, and E. N. Brown, "Dynamic analysis of learning in behavioral experiments," *J. Neurosci.*, vol. 24, no. 2, pp. 447–461, 2004.

[60] A. L. Goldberger, L. A. N. Amaral, L. Glass, J. M. Hausdorff, P. C. Ivanov, R. G. Mark, J. E. Mietus, G. B. Moody, C.-K. Peng, and H. E. Stanley, "PhysioBank, PhysioToolkit, and PhysioNet: Components of a new research resource for complex physiologic signals," *Circulation*, vol. 101, no. 23, pp. e215–e220, Jun. 2000.

[61] D. S. Wickramasuriya and R. T. Faghih, "A Bayesian filtering approach for tracking arousal from binary and continuous skin conductance features," *IEEE Trans. Biomed. Eng.*, vol. 67, no. 6, pp. 1749–1760, Jun. 2020.

[62] R. Atchley, R. Ellingson, D. Klee, T. Memmott, and B. Oken, "A cognitive stressor for event-related potential studies: The portland arithmetic stress task," *Stress*, vol. 20, no. 3, pp. 277–284, May 2017.

[63] S. Sharma, S. Rewadkar, H. Pawar, V. Deokar, and V. M. Lomte, "Survey on binaural beats and background music for increased focus and relaxation," in *Proc. Int. Conf. Emerg. Trends Innov. ICT (ICEI)*, Feb. 2017, pp. 98–103.

[64] R. Nawaz, H. Nisar, and Y. V. Voon, "The effect of music on human brain; frequency domain and time series analysis using electroencephalogram," *IEEE Access*, vol. 6, pp. 45191–45205, 2018.

[65] W. Boucsein, *Electrodermal Activity*. New York, NY, USA: Springer, 2012.

[66] J. M. Mendel, *Lessons in Estimation Theory for Signal Processing, Communications, and Control*. London, U.K.: Pearson, 1995.

[67] P. Geladi and B. R. Kowalski, "Partial least-squares regression: A tutorial," *Anal. Chim. Acta*, vol. 185, pp. 1–17, Jan. 1986.

[68] G. Feng, "A survey on analysis and design of model-based fuzzy control systems," *IEEE Trans. Fuzzy Syst.*, vol. 14, no. 5, pp. 676–697, Oct. 2006.

[69] M. Neumann-Brosig, A. Marco, D. Schwarzmann, and S. Trimpe, "Data-efficient autotuning with Bayesian optimization: An industrial control study," *IEEE Trans. Control Syst. Technol.*, vol. 28, no. 3, pp. 730–740, May 2020.

[70] J. Vinogradska, B. Bischoff, D. Nguyen-Tuong, A. Romer, H. Schmidt, and J. Peters, "Stability of controllers for Gaussian process forward models," in *Proc. Int. Conf. Mach. Learn.*, 2016, pp. 545–554.

[71] J. Steinhardt and R. Tedrake, "Finite-time regional verification of stochastic non-linear systems," *Int. J. Robot. Res.*, vol. 31, no. 7, pp. 901–923, Jun. 2012.

[72] F. Blanchini, "Set invariance in control," *Automatica*, vol. 35, no. 11, pp. 1747–1767, Nov. 1999.

[73] A. Greco, G. Valenza, and E. P. Scilingo, "Evaluation of cda and cvxeda models," in *Advances in Electrodermal Activity Processing With Applications for Mental Health*. Cham, Switzerland: Springer, 2016, pp. 35–43.

[74] J. Ponsford, N. K. Lee, D. Wong, A. McKay, K. Haines, Y. Alway, M. Downing, C. Furtado, and M. L. O'Donnell, "Efficacy of motivational interviewing and cognitive behavioral therapy for anxiety and depression symptoms following traumatic brain injury," *Psychol. Med.*, vol. 46, no. 5, pp. 1079–1090, Apr. 2016.

[75] D. Nie, X.-W. Wang, L.-C. Shi, and B.-L. Lu, "EEG-based emotion recognition during watching movies," in *Proc. 5th Int. IEEE/EMBS Conf. Neural Eng.*, Apr. 2011, pp. 667–670.

[76] X. Hou, Y. Liu, O. Sourina, Y. R. E. Tan, L. Wang, and W. Mueller-Wittig, "EEG based stress monitoring," in *Proc. IEEE Int. Conf. Syst., Man, Cybern.*, Oct. 2015, pp. 3110–3115.

[77] D. S. Wickramasuriya and R. T. Faghih, "A mixed filter algorithm for sympathetic arousal tracking from skin conductance and heart rate measurements in pavlovian fear conditioning," *PLoS ONE*, vol. 15, no. 4, Apr. 2020, Art. no. e0231659.

[78] P. Pohjavaara, T. Telaranta, and E. Väisänen, "The role of the sympathetic nervous system in anxiety: Is it possible to relieve anxiety with endoscopic sympathetic block?" *Nordic J. Psychiatry*, vol. 57, no. 1, pp. 55–60, Jan. 2003.

[79] T. Hollenstein, A. McNeely, J. Eastabrook, A. Mackey, and J. Flynn, "Sympathetic and parasympathetic responses to social stress across adolescence," *Develop. Psychobiol.*, vol. 54, no. 2, pp. 207–214, Mar. 2012.

[80] B. van der Vijgh, R. J. Beun, M. van Rood, and P. Werkhoven, "GASICA: Generic automated stress induction and control application design of an application for controlling the stress state," *Frontiers Neurosci.*, vol. 8, p. 400, Dec. 2014.

[81] A. Bernier, S. M. Carlson, S. Bordeleau, and J. Carrier, "Relations between physiological and cognitive regulatory systems: Infant sleep regulation and subsequent executive functioning," *Child Develop.*, vol. 81, no. 6, pp. 1739–1752, Nov. 2010.

[82] J. Umlauft, L. Pohler, and S. Hirche, "An uncertainty-based control Lyapunov approach for control-affine systems modeled by Gaussian process," *IEEE Control Syst. Lett.*, vol. 2, no. 3, pp. 483–488, Jul. 2018.

[83] S. Li, C. K. Ahn, and Z. Xiang, "Command-filter-based adaptive fuzzy finite-time control for switched nonlinear systems using state-dependent switching method," *IEEE Trans. Fuzzy Syst.*, vol. 29, no. 4, pp. 833–845, Apr. 2021.

[84] F. A. Russo, N. N. Vempala, and G. M. Sandstrom, "Predicting musically induced emotions from physiological inputs: Linear and neural network models," *Frontiers Psychol.*, vol. 4, p. 468, Aug. 2013.

[85] E. M. Sokhadze, "Effects of music on the recovery of autonomic and electrocortical activity after stress induced by aversive visual stimuli," *Appl. Psychophysiol. Biofeedback*, vol. 32, no. 1, pp. 31–50, Mar. 2007.

[86] L. Stewart, "Editorial," *Psychomusicol., Music, Mind, Brain*, vol. 22, no. 2, p. 95, 2012.

[87] S. Khalfa, P. Isabelle, B. Jean-Pierre, and R. Manon, "Event-related skin conductance responses to musical emotions in humans," *Neurosci. Lett.*, vol. 328, no. 2, pp. 145–149, Aug. 2002.

[88] L. Wilms and D. Oberfeld, "Color and emotion: Effects of hue, saturation, and brightness," *Psychol. Res.*, vol. 82, no. 5, pp. 896–914, Sep. 2018.

[89] P. Zieli ski, "An arousal effect of colors saturation: A study of self-reported ratings and electrodermal responses," *J. Psychophysiol.*, vol. 30, no. 1, pp. 9–16, Jan. 2016.

[90] R. J. Rajae-Joordens, "The effects of colored light on valence and arousal," in *Sensing Emotions* (Philips Research Book Series), vol. 12. Dordrecht, The Netherlands: Springer, 2010, pp. 65–84.

[91] A. Toet, S. Eijsman, Y. Liu, S. Donker, D. Kaneko, A.-M. Brouwer, and J. B. F. van Erp, "The relation between valence and arousal in subjective odor experience," *Chemosensory Perception*, vol. 13, no. 2, pp. 141–151, Oct. 2020.

[92] C. Beyts, C. Chaya, F. Dehrmann, S. James, K. Smart, and J. Hort, "A comparison of self-reported emotional and implicit responses to aromas in beer," *Food Qual. Preference*, vol. 59, pp. 68–80, Jul. 2017.

[93] R. S. Herz, "Influences of odors on mood and affective cognition," *Olfaction, Taste, Cognition*, vol. 160, p. 177, Oct. 2002.

[94] P. T. Quinlan, J. Lane, K. L. Moore, J. Aspen, J. A. Rycroft, and D. C. O'Brien, "The acute physiological and mood effects of tea and coffee: The role of caffeine level," *Pharmacol. Biochemistry Behav.*, vol. 66, no. 1, pp. 19–28, 2000.

[95] A. Lemercier-Talbot, G. Coppin, D. Cereghetti, C. Porcherot, I. Cayeux, and S. Delplanque, "Measuring automatic associations between relaxing/energizing feelings and odors," *Food Qual. Preference*, vol. 77, pp. 21–31, Oct. 2019.

[96] S. Nirjon, F. Zhao, R. F. Dickerson, Q. Li, P. Asare, J. A. Stankovic, D. Hong, B. Zhang, X. Jiang, and G. Shen, "MusicalHeart: Aheartyway of listening to music," in *Proc. 10th ACM Conf. Embedded Netw. Sensor Syst. (SenSys)*, 2012, pp. 43–56.

[97] K. Markov, T. Matsui, F. Septier, and G. Peters, "Dynamic speech emotion recognition with state-space models," in *Proc. 23rd Eur. Signal Process. Conf. (EUSIPCO)*, Aug. 2015, pp. 2077–2081.

[98] S. Ntalampiras and I. Potamitis, "A statistical inference framework for understanding music-related brain activity," *IEEE J. Sel. Topics Signal Process.*, vol. 13, no. 2, pp. 275–284, May 2019.

[99] S. Lui and D. Grunberg, "Using skin conductance to evaluate the effect of music silence to relieve and intensify arousal," in *Proc. Int. Conf. Orange Technol. (ICOT)*, Dec. 2017, pp. 91–94.

[100] A. Linnemann, M. Wenzel, J. Grammes, T. Kubiak, and U. M. Nater, "Music listening and stress in daily life—A matter of timing," *Int. J. Behav. Med.*, vol. 25, no. 2, pp. 223–230, 2018.

[101] H. Liang, J. Zou, K. Zuo, and M. J. Khan, "An improved genetic algorithm optimization fuzzy controller applied to the wellhead back pressure control system," *Mech. Syst. Signal Process.*, vol. 142, Aug. 2020, Art. no. 106708.

[102] D. M. Alexander, C. Trengove, P. Johnston, T. Cooper, J. P. August, and E. Gordon, "Separating individual skin conductance responses in a short interstimulus-interval paradigm," *J. Neurosci. Methods*, vol. 146, no. 1, pp. 116–123, Jul. 2005.

[103] M. Benedek and C. Kaernbach, "Decomposition of skin conductance data by means of nonnegative deconvolution," *Psychophysiology*, vol. 47, no. 4, pp. 647–658, Jul. 2010.

[104] R. T. Faghih, M. A. Dahleh, G. K. Adler, E. B. Klerman, and E. N. Brown, "Deconvolution of serum cortisol levels by using compressed sensing," *PLoS ONE*, vol. 9, no. 1, Jan. 2014, Art. no. e85204.

HAMID FEKRI AZGOMI (Student Member, IEEE) received the B.S. degree in electrical engineering from Imam Khomeini International University, Qazvin, Iran, in 2010, and the M.S. degree in electrical engineering from the Iran University of science and Technology, Tehran, Iran, in 2013. He is currently pursuing the Ph.D. degree in electrical engineering with the University of Houston, Houston, TX, USA.

His current research interests include physiological signal processing and closed-loop control with an emphasis on biomedical applications and neuroscience.

IAHN CAJIGAS (Member, IEEE) received the B.S. and M.Eng. degrees in electrical engineering and computer science from the Massachusetts Institute of Technology (MIT), Cambridge, MA, USA, in 2002 and 2003, respectively, and the Ph.D. degree in medical and electrical engineering from the Harvard-MIT Division of Health Sciences and Technology under the joint supervision of Emery N. Brown (M.D. and Ph.D. at MIT) and Paolo Bonato (Ph.D. at Spaulding Rehabilitation Hospital, Harvard Medical School, in 2012).

He completed medical school training at Harvard Medical School, in 2014, as part of the Harvard M.D.-Ph.D. Program and the joint Harvard-MIT Division of Health Science and Technology. He is currently completing his training in neurological surgery at the University of Miami/Jackson Memorial Hospital. He is currently the Chief Resident with the Department of Neurosurgery, University of Miami/Jackson Memorial Hospital. During his residency training, he completed an enfolded fellowship in functional and stereotactic neurosurgery and has worked on the development of models of laser thermal therapy for the treatment of drug-resistant epilepsy and brain tumors. His clinical interests include the surgical management of epilepsy, novel treatment paradigms for spinal cord injury, and deep brain stimulation for movement disorders.

Dr. Caijigas was awarded the MIT Presidential Fellowship along with an NIH F31 Predoctoral Fellowship for his doctoral research. He was recently awarded the NIH R25 for his research on brain machine interfaces for the control of hand grasp in patients with spinal cord injury.

ROSE T. FAGHIH (Member, IEEE) received the B.S. degree *(summa cum laude)* in electrical engineering from the University of Maryland, College Park, MD, USA, in 2008, and the S.M. and Ph.D. degrees in electrical engineering and computer science (mathematics) from the Massachusetts Institute of Technology (MIT), Cambridge, MA, USA, in 2010 and 2014, respectively.

She is currently an Assistant Professor with the Department of Electrical and Computer Engineering, University of Houston, where she directs the Computational Medicine Laboratory. She completed her postdoctoral training at the Department of Brain and Cognitive Sciences, The Picower Institute for Learning and Memory, MIT, and the Department of Anesthesia, Critical Care and Pain Medicine, Massachusetts General Hospital. At MIT, she was with the Laboratory for Information and Decision Systems and the MIT-Harvard Neuroscience Statistics Research Laboratory. Her research interests include wearable technologies, medical cyber-physical systems, control, estimation, and system identification of biomedical and neural systems.

Dr. Faghih was a recipient of various awards, including the MIT Technology Review 2020 Innovator Under 35 awards, the 2020 National Science Foundation (NSF) CAREER Award, the 2020 Research Excellence Award and the 2020 Teaching Excellence Award from the University of Houston's Cullen College of Engineering, the 2016 IEEE-USA New Face of Engineering Award, the National Science Foundation Graduate Research Fellowship, the MIT Graduate Fellowship, and the University of Maryland's Department of Electrical and Computer Engineering Chair's Award. She has also been inducted into various honor societies, including Phi Kappa Phi, Tau Beta Pi, and Eta Kappa Nu.